Figure 1. (A) 'O-Acyl isopeptide method': the synthetic strategy for difficult sequence-containing peptides via the O–N intramolecular acyl migration reaction of O-acyl isopeptides, (B) application of the O-acyl isopeptide method for the synthesis of pentapeptides 1 and 3.
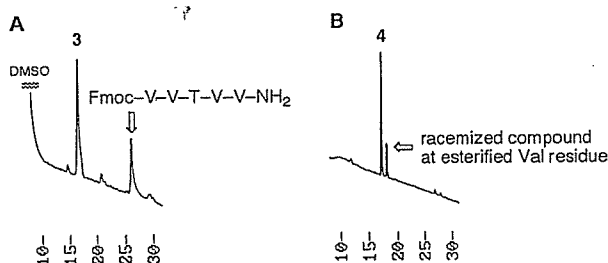

Figure 2. HPLC profiles of crude (A) peptide 3 (synthesized by the standard SPPS) and (B) its O-acyl isopeptide 4. Analytical HPLC was performed using a C18 reverse phase column (4.6 × 150 mm; YMC Pack ODS AM302) with a binary solvent system: a linear gradient of CH_3CN (0–100% CH_3CN, 40 min) in 0.1% aqueous TFA at a flow rate of 0.9 mL min^{-1} (40 °C), detected at 230 nm.

DMSO solution of 3 was used for HPLC purification, the overall yield of 3 was only 1.4%.[4]

For the case of O-acyl isopeptide method,[5] Boc-Thr-OH was coupled to the H-Val-Val-NH-resin, and subsequent acylation with Fmoc-Val-OH to the β-hydroxyl group of Thr was performed using the DIPCDI–DMAP method in CH_2Cl_2 to obtain ester. After coupling with another Val residue, N-acetylation and TFA treatment, O-acyl isopeptide 4·TFA was obtained without forming Fmoc-containing by-product (Fig. 2B). Hence, the protected peptide resin was efficiently synthesized with no interference from the difficult sequences. The results support our hypothesis, that the modification of 3 to the ester structure 4 changed the secondary structure of peptide to that more favorable for Fmoc-deprotection. Moreover, the solubility of 4·TFA in H_2O or MeOH was 46.2 ± 22.7 (5775-fold) or 266.5 ± 65.4 (4517-fold) mg mL^{-1}, respectively, higher than that of N-acyl peptide 3, because of the ionized amino group in the isopeptide. Accordingly, a solution of 4·TFA in MeOH could easily be applied to preparative HPLC,

and 4·TFA was purified using the 0.1% aqueous TFA–CH_3CN system as the eluant to obtain pure 4 with an isolated yield of 28.0%.

However, a large amount of racemization (21%) of the esterified Val residue occurred in the DIPCDI–DMAP method (Fig. 2B), which was confirmed by an independent synthesis of H-Thr(Ac-Val-D-Val)-Val-Val-NH_2. This extent of racemization is remarkably higher than that of the esterification between Val and Ser in 2 (0.8%),[2b,d,e] which is probably due to steric hindrance at the secondary hydroxyl group in Thr as compared to Ser. We also observed a slightly higher amount of racemization (33%) when 1-(mesitylene-2-sulfonyl)-3-nitro-1,2,4-triazole (MSNT) (3.0 equiv)–N-methylimidazole (NMI) (12 equiv) in CH_2Cl_2[6] was used for the esterification, which agrees with a literature report.[6c] We considered that the large extent of racemization should be a serious disadvantage in the synthesis of Thr-containing peptides using the O-acyl isopeptide method.

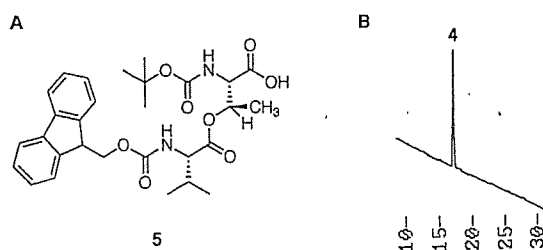To avoid this problem, we decided to adapt an O-acyl isodipeptide unit, Boc-Thr(Fmoc-Val)-OH 5 (Fig. 3A),

Figure 3. (A) O-Acyl isodipeptide unit 5 and (B) crude isopeptide 4 (synthesized using 5). Analytical HPLC was performed using a C18 reverse phase column (4.6 × 150 mm; YMC Pack ODS AM302) with binary solvent system: a linear gradient of CH_3CN (0–100% CH_3CN, 40 min) in 0.1% aqueous TFA at a flow rate of 0.9 mL min^{-1} (40 °C), detected at 230 nm.
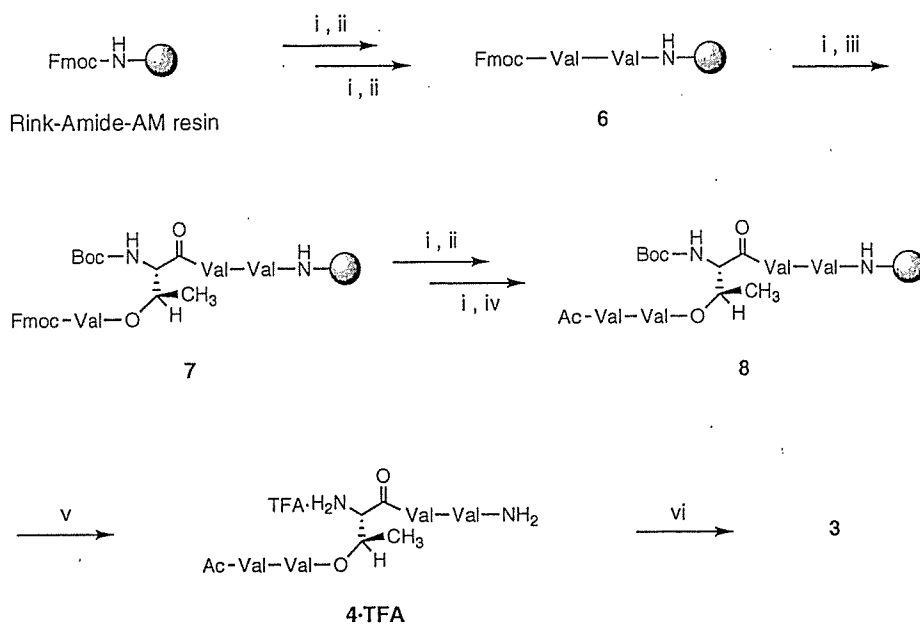
Scheme 1. Reagents and conditions: (i) 20% piperidine/DMF, 20 min; (ii) Fmoc-Val-OH (2.5 equiv), DIPCDI (1,3-diisopropylcarbodiimide, 2.5 equiv), HOBt (2.5 equiv), DMF, 2 h; (iii) 5 (2.5 equiv), DIPCDI (2.5 equiv), HOBt (2.5 equiv), DMF, 2 h; (iv) Ac$_2$O (1.5 equiv), TEA (1.0 equiv), DMF, 2 h; (v) TFA–m-cresol–thioanisole–H$_2$O (92.5:2.5:2.5:2.5), 90 min; (vi) phosphate buffered saline (PBS), pH 7.4, 25 °C.

which was synthesized by solution phase,[7] for the synthesis of 3 based on the O-acyl isopeptide method (Scheme 1).[8] The use of isodipeptide 5 could omit the racemization-inducing esterification reaction. The O-acyl isodipeptide 5, which readily solubilized in DMF, was coupled to the H-Val-Val-NH-resin using the standard DIPCDI–HOBt method (2 h) to obtain 7. The completeness of the coupling was verified by the Keiser test. After coupling with another Val residue followed by N-acetylation and TFA–m-cresol–thioanisole–H$_2$O (92.5:2.5:2.5:2.5) treatment, O-acyl isopeptide 4·TFA was obtained. As shown in Figure 3B, HPLC analysis of crude 4 (synthesized using O-acyl isodipeptide unit 5) exhibited a high purity of the desired product 4 with no by-product derived from the difficult sequence or racemization. The use of isodipeptide 5 did not lead to any additional side reaction. Moreover, since H-Thr-Val-Val-NH$_2$ was not formed as a by-product, we concluded that (1) the ester bond between Val and Thr was stable in both piperidine and TFA treatments and (2) diketopiperazine was not formed when the last Fmoc group was removed. Consequently, we could obtain pure 4 without further purification, with an isolated yield of 44.5%.

Compound 4·TFA was stable at 4 °C for at least 2 years. On the other hand, when 4·TFA was dissolved and stirred in phosphate buffered saline (PBS, pH 7.4) at rt, quantitative O–N intramolecular acyl migration to the corresponding parent peptide 3 was observed with no side reaction (Fig. 4A).[9] Isopeptide 4 exhibited more than 5-fold faster migration with a half-life of 23 min than that observed in 2 containing Ser (half-life = 2 h).[2b,d,e] The faster migration in 4 may be attributed to a unique interlocking effect of the β-methyl group in Thr, which has conformational restrictions, such as
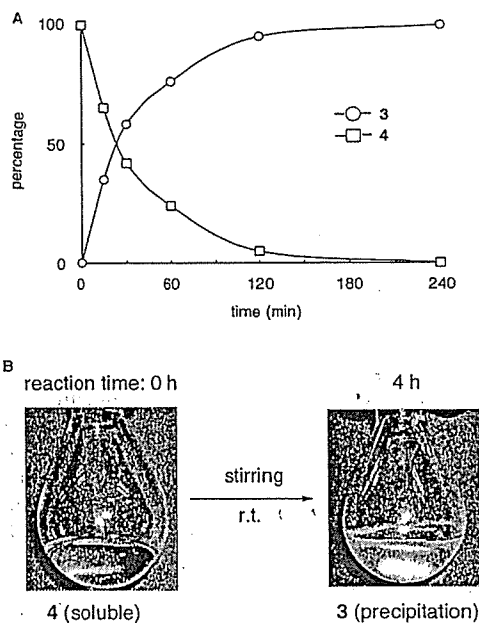

Figure 4. (A) A graph and (B) photographs in conversion of O-acyl isopeptide 4 to 3 via the O–N intramolecular acyl migration in phosphate buffered saline (pH 7.4, 25 °C).

a gem-effect by geminal methyl substitution.[10] Finally, as depicted in Figure 4B, 3 was formed as a white precipitate from 4. The resulting precipitate was centrifuged and washed with water and methanol to afford highly pure 3. The overall yield of 3 in O-acyl isopeptide method was 42.7%.[8]

In conclusion, 'O-acyl isopeptide method' with a novel O-acyl isodipeptide unit, Boc-Thr(Fmoc-Val)-OH 5, in which the racemization-inducing esterification reaction

could be omitted, has been successfully applied to the efficient synthesis of a difficult sequence-containing pentapeptide by improving the nature of difficult sequence during SPPS. This suggests that the use of *O*-acyl isodipeptide units allows the application of '*O*-acyl isopeptide method' to fully automated protocols for the synthesis of long peptides or proteins.

Acknowledgments

References and notes

1. (a) Wöhr, T.; Wahl, F.; Nefzi, A.; Rohwedder, B.; Sato, T.; Sun, X.; Mutter, M. *J. Am. Chem. Soc.* **1996**, *118*, 9218–9227; For a review, see: (b) Sheppard, R. *J. Pept. Sci.* **2003**, *9*, 545–552.
2. (a) Sohma, Y.; Sasaki, M.; Ziora, Z.; Takahashi, N.; Kimura, T.; Hayashi, Y.; Kiso, Y. *Peptides, Peptide Revolution: Genomics, Proteomics & Therapeutics*; Kluwer Academic: Netherlands, 2003; pp 67–68; (b) Sohma, Y.; Sasaki, M.; Hayashi, Y.; Kimura, T.; Kiso, Y. *Chem. Commun.* **2004**, 124–125; (c) Sohma, Y.; Sasaki, M.; Hayashi, Y.; Kimura, T.; Kiso, Y. *Tetrahedron Lett.* **2004**, *45*, 5965–5968; (d) Sohma, Y.; Hayashi, Y.; Skwarczynski, M.; Hamada, Y.; Sasaki, M.; Kimura, T.; Kiso, Y. *Biopolymers* **2004**, *76*, 344–356; (e) Sohma, Y.; Hayashi, Y.; Kimura, M.; Chiyomori, Y.; Taniguchi, A.; Sasaki, M.; Kimura, T.; Kiso, Y. *J. Pept. Sci.* **2005**, *11*, 441–451; (f) Sohma, Y.; Chiyomori, Y.; Kimura, M.; Fukao, F.; Taniguchi, A.; Hayashi, Y.; Kimura, T.; Kiso, Y. *Bioorg. Med. Chem.* **2005**, *13*, 6167–6174; (g) Taniguchi, A.; Sohma, Y.; Kimura, M.; Okada, T.; Ikeda, K.; Hayashi, Y.; Kimura, T.; Hirota, S.; Matsuzaki, K.; Kiso, Y. *J. Am. Chem. Soc.* **2006**, *128*, 696–697.
3. (a) Mutter, M.; Chandravarkar, A.; Boyat, C.; Lopez, J.; Santos, S. D.; Mandal, B.; Mimna, R.; Murat, K.; Patiny, L.; Saucède, L.; Tuchscherer, G. *Angew. Chem., Int. Ed.* **2004**, *43*, 4172–4178; (b) Carpino, L. A.; Krause, E.; Sferdean, C. D.; Schümann, M.; Fabian, H.; Bienert, M.; Beyermann, M. *Tetrahedron Lett.* **2004**, *45*, 7519–7523; (c) Santos, S. D.; Chandravarkar, A.; Mandal, B.; Mimna, R.; Murat, K.; Saucède, L.; Tella, P.; Tuchscherer, G.; Mutter, M. *J. Am. Chem. Soc.* **2005**, *127*, 11888–11889.
4. The peptide 3 was synthesized on Rink amide aminomethyl (AM) resin (200 mg, 0.126 mmol) according to the general Fmoc-based solid-phase procedure. After the resin was washed with DMF (1.5 mL, ×5), Fmoc-Val-OH (107 mg, 0.315 mmol), and Fmoc-Thr(*t*Bu)-OH (111 mg, 0.315 mmol) were coupled in the presence of 1,3-diisopropylcarbodiimide (DIPCDI, 49.2 µL, 0.315 mmol) and 1-hydroxybenzotriazole (HOBt, 48.2 mg, 0.315 mmol) in

DMF (1.5 mL) for 2 h according to the sequence. The Fmoc-group was removed by 20% piperidine/DMF (20 min). *N*-Acetylation was carried out with Ac$_2$O (14.3 µL, 0.151 mmol) in the presence of TEA (17.5 µL, 0.126 mmol) for 2 h. The peptide was cleaved from the resin using TFA (4.7 mL) in the presence of thioanisole (126 µL), *m*-cresol (126 µL), and distilled water (126 µL) for 90 min at rt, concentrated in vacuo, washed with Et$_2$O, centrifuged, suspended with water, and lyophilized to give the crude peptide (45.9 mg). This crude peptide (20 mg) was saturated in DMSO, filtered using a 0.46 µm filter unit, and immediately injected into preparative HPLC with a 0.1% aqueous TFA–CH$_3$CN system. The desired fractions were collected and immediately lyophilized to afford the desired peptide 3 as a white amorphous powder. Yield: 0.4 mg (1.4%); HRMS (FAB): calcd for C$_{26}$H$_{49}$N$_6$O$_7$ (M+H)$^+$: 557.3663, found: 557.3657; HPLC analysis at 230 nm: purity was higher than 95%.
5. After the preparation of the H-Val-Val-NH-resin (Rink amide AM resin, 200 mg, 0.126 mmol) in the same manner as described in the synthesis of 3 using the conventional method, Boc-Thr-OH (82.9 mg, 0.378 mmol) was coupled in the presence of DIPCDI (59.2 µL, 0.378 mmol) and HOBt (57.8 mg, 0.378 mmol) in DMF (1.5 mL). Subsequent coupling with Fmoc-Val-OH (128 mg, 0.378 mmol) to the β-hydroxyl group of Thr was performed using the DIPCDI (59.2 µL, 0.378 mmol)–DMAP (3.1 mg, 0.0252 mmol) method in CH$_2$Cl$_2$ (1.5 mL) for 16 h (×2), followed by coupling with another Val residue, *N*-acetylation using Ac$_2$O (17.8 µL, 0.15 mmol)–TEA (17.6 µL, 0.126 mmol), TFA (4.7 mL)–thioanisole (128 µL)–*m*-cresol (128 µL)–distilled water (128 µL) treatment for 90 min at rt, concentration in vacuo, Et$_2$O wash, centrifugation, suspension in water, and lyophilization to give the crude *O*-acyl isopeptide 4·TFA (51.5 mg). This crude peptide (20 mg) was dissolved in MeOH, filtered using a 0.46 µm filter unit, and immediately injected into preparative HPLC with a 0.1% aqueous TFA–CH$_3$CN system. The desired fractions were collected and immediately lyophilized, affording the desired *O*-acyl isopeptide 4·TFA as a white amorphous powder (9.2 mg, 28.0%). HRMS (FAB): calcd for C$_{26}$H$_{49}$N$_6$O$_7$ (M+H)$^+$: 557.3663, found: 557.3666; HPLC analysis at 230 nm: purity was higher than 95%.
6. (a) Nielsen, J.; Lyngso, L. O. *Tetrahedron Lett.* **1996**, *37*, 8439–8442; (b) Meldal, M.; Svendsen, I. B.; Juliano, L.; Juliano, M. A.; Del, N. E.; Scharfstein, J. *J. Pept. Sci.* **1998**, *4*, 83–91; (c) Tamamura, H.; Kato, T.; Otaka, A.; Fujii, N. *Org. Biomol. Chem.* **2003**, *1*, 2468–2473.
7. EDC·HCl (104 mg, 0.539 mmol) was added to a stirring solution of *N*-(*t*-butoxycarbonyl)-L-threonine benzyl ester (Boc-Thr-OBzl)^{11} (139 mg, 0.449 mmol), *N*-(9*H*-fluoren-9-ylmethoxycarbonyl)-L-valine (Fmoc-Val-OH, 183 mg, 0.539 mmol), and DMAP (5.5 mg, 0.045 mmol) in dry CHCl$_3$ (10 mL) at 0 °C. The mixture was slowly warmed to rt over 2 h, stirred additionally for 5 h, diluted with AcOEt, and washed successively with water, 1 M HCl, water, a saturated NaHCO$_3$, and brine. The organic layer was dried over MgSO$_4$ and the solvent was removed in vacuo. The resulting oil was purified by silica gel column chromatography (AcOEt–hexane 1:4) to yield Boc-Thr(Fmoc-Val)-OBzl (266 mg, 0.422 mmol, 94%). Epimerization during the above reaction was not detected, which was confirmed by comparison with independently synthesized D-valine derivative. After that, Pd/C was added (12 mg) to the stirring solution of the Boc-Thr(Fmoc-Val)-OBzl (236 mg, 0.374 mmol) in AcOEt (10 mL), and the reaction mixture was vigorously stirred for 3 h (it is worthy to notice that the higher amount of

Pd/C caused by-products formation). The catalyst was filtered off through Celite. The solvent was removed in vacuo and the crude product was filtered via silica gel, at first with AcOEt–hexane 1:2 and then the final product was washed out by methanol to give pure **5** (186 mg, 0.346 mmol, 92%). HRMS (FAB): calcd for $C_{29}H_{36}$-N_2O_8Na (M+Na)$^+$: 563.2369, found: 563.2373; HPLC analysis at 230 nm: purity was higher than 95%; NMR (CD$_3$OD, 400 MHz): δ 7.79 (d, ^3J(H,H) = 7.3 Hz, 2H, CH), 7.75–7.66 (m, 2H, CH), 7.38 (t, ^3J(H,H) = 7.5 Hz, 2H, CH), 7.33–7.29 (m, 2H, CH), 5.44–5.41 (m, 1H, CH), 4.38 (d, ^3J(H,H) = 7.0 Hz, 2H, CH$_2$), 4.25–4.22 (m, 2H, CH), 4.05–4.01 (m, 1H, CH), 2.11–2.02 (m, 1H, CH), 1.44 (s, 9H, CH$_3$), 1.25 (d, ^3J(H,H) = 6.4 Hz, 3H, CH$_3$), 0.91, 0.89 (2d, ^3J(H,H) = 7.7, 7.0 Hz, 6H, CH$_3$).

8. After the preparation of the H-Val-Val-NH-resin (Rink amide AM resin, 100 mg, 0.071 mmol) in the same manner described in the synthesis of **3** using the conventional method, Boc-Thr(Fmoc-Val)-OH **5** (100 mg, 0.18 mmol) was coupled in the presence of DIPCDI (29.0 μL, 0.18 mmol) and HOBt (28.4 mg, 0.18 mmol) in DMF (1.5 mL). Subsequent coupling with Fmoc-Val-OH (62.8 mg, 0.18 mmol), *N*-acetylation using Ac$_2$O (10.5 μL, 0.11 mmol)–TEA (10.4 μL, 0.071 mmol), TFA (2.47 mL)–thioanisole (66.7 μL)–*m*-cresol (66.7 μL)–distilled water (66.7 μL) treatment for 90 min at rt, concentration in vacuo, Et$_2$O wash, centrifugation, suspension in water, and lyophilization gave the pure *O*-acyl isopeptide **4**·TFA as a white amorphous powder (21.2 mg, 44.5%). HRMS (FAB): calcd for $C_{26}H_{49}N_6O_7$ (M+H)$^+$: 557.3663,

found: 557.3666; HPLC analysis at 230 nm: purity was higher than 95%. Purified *O*-acyl isopeptide **4**·TFA (3.0 mg) was then dissolved in phosphate-buffered saline (PBS, pH 7.4, 3 mL) at rt and stirred overnight at rt. The resultant precipitate was centrifuged and washed with water and MeOH followed by drying in vacuo to give **3** as a white powder. Yield: 2.4 mg (96%); HRMS (FAB): calcd for $C_{26}H_{49}N_6O_7$ (M+H)$^+$: 557.3663, found: 557.3667; HPLC analysis at 230 nm: purity was higher than 95%; the retention time on HPLC (0–100% CH$_3$CN for 40 min, 230 nm) of synthesized product was identical to that of **3**, which was synthesized independently by the conventional method.[4]

9. To PBS (495 μL, pH 7.4) were added DMSO (4 μL) and solution of **4** (1 μL, 10 mM in DMSO), and the mixture was stirred at rt. At the desired time points, DMSO (500 μL) was added to the samples and the mixture was directly analyzed by RP-HPLC. HPLC was performed using a C18 (4.6 × 150 mm; YMC Pack ODS AM302) reverse-phase column with a binary solvent system: linear gradient of CH$_3$CN (0–100%, 40 min) in 0.1% aqueous TFA at a flow rate of 0.9 mL min^{-1}, detected at UV 230 nm.

10. (a) Beesley, R. M.; Ingold, C. K.; Thorpe, J. F. *J. Chem. Soc.* **1915**, *107*, 1080–1106; (b) Matsumoto, H.; Sohma, Y.; Kimura, T.; Hayashi, Y.; Kiso, Y. *Bioorg. Med. Chem. Lett.* **2001**, *11*, 605–609.

11. Skwarczynski, M.; Sohma, Y.; Noguchi, M.; Hayashi, Y.; Kimura, T.; Kiso, Y. *J. Org. Chem.* **2006**, *71*, 2542–2545.

今エイズ薬研究はどうなっているか
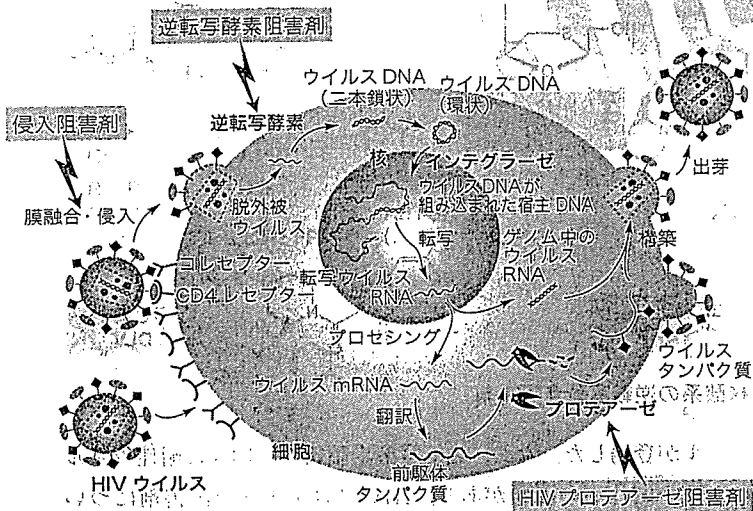
図1　HIVウイルスの生活環と対する抗HIV薬

日高興士[1]・木曽良明[2]
1 京都薬科大学21世紀COEプログラム，
2 京都薬科大学大学院薬学研究科，
　創薬科学フロンティア研究センター

日本を脅かすHIV

エイズ治療に抗HIV薬の多剤併用療法（highly active anti-retroviral therapy；HAART）が用いられるようになり，エイズによる死亡率や，それに関連する日和見感染症の発症率が劇的に低下した．しかし，HIVは体内から完全に除去できないこともわかり，一生涯という長期間にわたるウイルス制御による副作用や耐性ウイルスをいかに克服するかが今後の大きな課題となっている．また，わが国では年間のHIV新規報告者数が2004年に続いて昨年も1000件を超え，先進国のなかで感染者が増えつづける唯一の国として，HIV感染

日高興士（ひだか　こおし）
＜所属＞京都薬科大学21世紀COEプログラム助手．＜出身大学＞甲南大学大学院自然科学研究科修士課程（1999年修了）．＜研究テーマ＞酵素阻害剤の構造最適化研究．＜趣味＞ランニング，チョコレートづくり

木曽良明（きそ　よしあき）
＜所属＞京都薬科大学教授（大学院薬学研究科，創薬科学フロンティア研究センター）．＜出身大学＞京都大学大学院薬学研究科博士課程（1973年単位取得退学）．＜研究テーマ＞ペプチドのコンフォメーションと分子認識活性との相関研究．＜趣味＞スポーツ観戦，音楽鑑賞

は社会的に大きな問題になっている．ここでは，現在臨床で使われている抗HIV薬の紹介と，最近の抗HIV薬開発の動向，HAARTに大きく貢献するHIVプロテアーゼ阻害剤の研究最前線について解説したい．

現在使用されているエイズ治療薬

現在，日本ではアメリカのHIV感染症治療ガイドライン（DHHS）[1]を参考にしたHIV感染症治療が行われており，国内のHIV診療医師がまとめた「治療の手引き」が毎年改訂されている[2]．HAARTに使用される薬剤には，核酸系および非核酸系の逆転写酵素阻害剤，HIVプロテアーゼ阻害剤，侵入阻害剤の3種類がある（図1）．ただし，侵入阻害剤はまだ日本では認可されていない．そのため，現在は患者のCD4陽性リンパ球数と血中ウイルス量に臨床症状を考慮したうえで，逆転写酵素阻害剤，HIVプロテアーゼ阻害剤のうちから3剤以上を併用する抗HIV療法が開始される．ちなみに最近は，1日1回（once daily）処方（1日1回の投与あるいは服用）[3]の薬剤が好まれつつある．

ここで，それぞれの薬剤について簡略に紹介したい．まず，核酸系の逆転写酵素阻害剤（図2上）は化学構造が核酸と同様で，細胞内でリン酸化されたあと，HIV逆転写酵素の基質と競合するかDNA鎖に取り込まれることでDNA鎖の伸長を阻害し，抗HIV活性を発現する．現在，この種の薬剤は八つあり，2005年にエムトリシタビン（商品名：エムトリバ）が国内

●核酸系●

ジドブジン AZT(ZDV)　ザルシタビン ddC　ジダノシン ddI　サニルブジン d4T　ラミブジン 3TC

アバカビル ABC　テノフォビル TDF　エムトリシタビン FTC

●非核酸系●

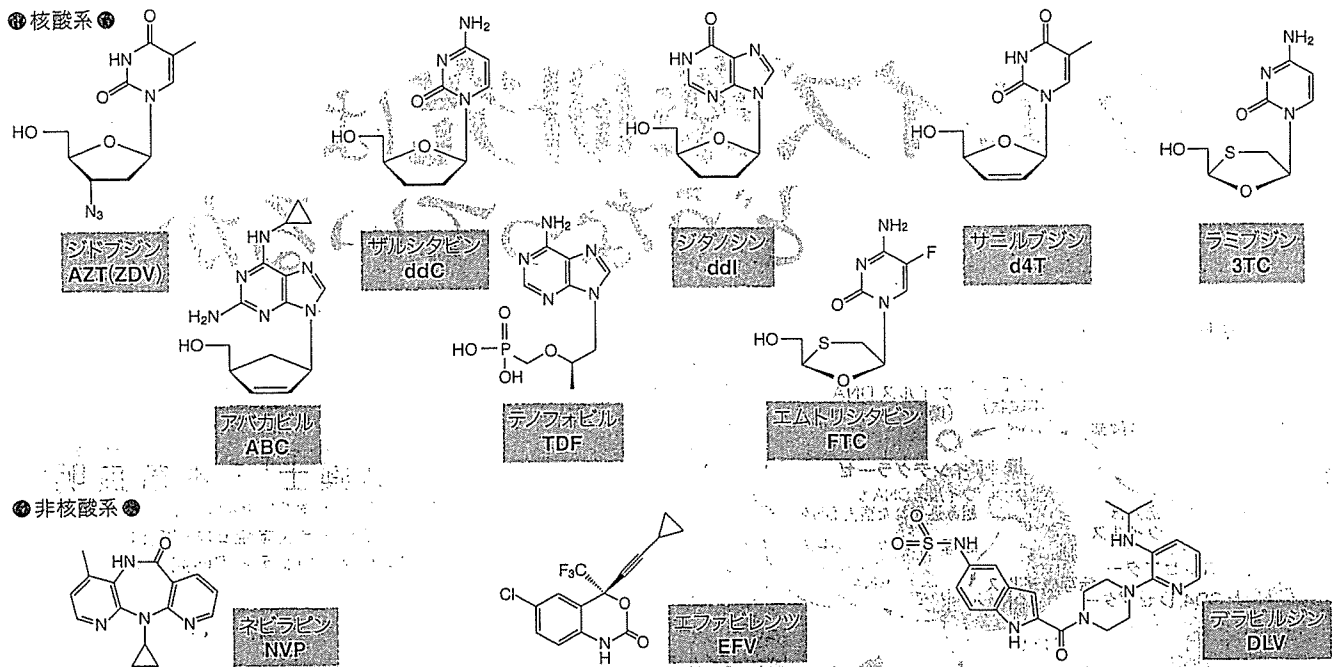ネビラピン NVP　エファビレンツ EFV　デラビルジン DLV

図2　核酸系および非核酸系の逆転写酵素阻害剤

で認可されたのは記憶に新しい．

この薬剤は血中濃度持続性が高く，1日1回の投与でよいものが多い．ただし，効力は優れているものの，耐性ウイルスや重篤な副作用（ミトコンドリア障害によるものらしい）が問題となっている．ミトコンドリア障害が少ないという点では，ヌクレオチド型のテノフォビル（商品名：ビリアード）が優れている．

非核酸系の逆転写酵素阻害剤（図2下）は，逆転写酵素の基質結合部位のごく近傍の部分に相互作用することでDNA鎖の伸長を阻害し，抗HIV活性を発現する．現在，日本では三つの薬剤が認可されている．1日1回投与のエファビレンツ（商品名：ストックリン）は抗ウイルス効果が優れており，初回治療の優先処方（未治療患者に施される治療で優先的に処方される薬）になっている．しかし，中枢神経系への副作用が指摘されている．また，非核酸系の逆転写酵素阻害剤は全般に，相互の交差耐性が問題となっている．

HIVプロテアーゼ阻害剤（図3）にはヒドロキシル基を含む基質遷移状態アナログが組み込まれており，プロテアーゼの活性中心に結合することで，翻訳されたHIV由来の前駆体タンパク質のプロセシングを阻害し，非感染性の未成熟ウイルスをつくらせることで抗HIV活性を発現する．現在は国内で八つの薬剤が多剤併用療法に使用され，そのうちカレトラ（ロピナビル・リトナビル配合剤）は治療効果に優れ，初回治療の優先処方である．また最近，1日1回服用のアタザナビ

ルが登場した．なお，逆転写酵素阻害剤と同様に耐性ウイルスや副作用の問題があるHIVプロテアーゼ阻害剤については，のちほど詳しく述べる．

そして，日本では認可されていないが，侵入阻害剤として，フュージョン（膜融合）阻害剤に分類されるエンフビルタイド（T-20）が唯一存在する．アミノ酸36残基からなるペプチド（acetyl- YTSLIHSLIEESQNQQEKNEQELLELDKWASLWNWF-NH₂）で，HIV表面糖タンパク質のgp41に結合し，ウイルスと細胞膜の融合に必須なgp41のループ構造形成を阻害して抗HIV活性を示す．多剤耐性株にも有効であることが期待されているが，1日2回の皮下注射が必要なことや薬価が非常に高額だという難点がある．

今，活発な研究テーマ

先に述べた阻害剤についての新規薬剤研究も進められているが，近年は侵入阻害剤およびインテグラーゼ阻害剤を主とした研究が活発に行われている．侵入阻害剤には，HIVが免疫細胞に侵入する際のHIV表面糖タンパク質gp120と宿主細胞表面のCD4との結合を標的にしたものや，コレセプターであるケモカイン受容体（CXCR4やCCR5）とCD4結合後の構造変化したgp120との結合を標的にしたもの，T-20のような細胞膜融合を標的にしたものがある．これら阻害剤のいくつかは現在臨床開発中であり，どれも宿主タンパク質が標的である
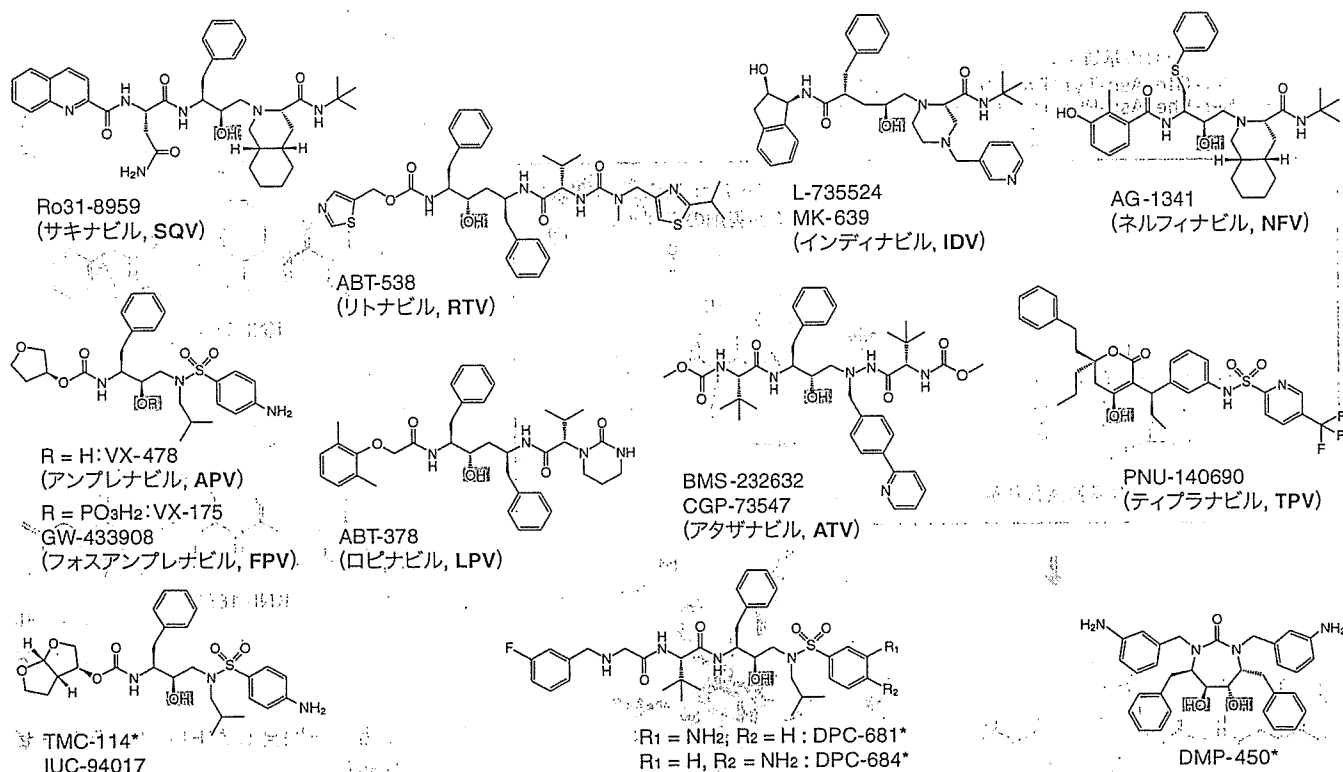
Ro31-8959
(サキナビル, SQV)

ABT-538
(リトナビル, RTV)

L-735524
MK-639
(インディナビル, IDV)

AG-1341
(ネルフィナビル, NFV)

R = H:VX-478
(アンプレナビル, APV)
R = PO₃H₂:VX-175
GW-433908
(フォスアンプレナビル, FPV)

ABT-378
(ロピナビル, LPV)

BMS-232632
CGP-73547
(アタザナビル, ATV)

PNU-140690
(ティプラナビル, TPV)

TMC-114*
IUC-94017

R₁ = NH₂, R₂ = H : DPC-681*
R₁ = H, R₂ = NH₂ : DPC-684*

DMP-450*

図 3 臨床適応および開発中 (*) の HIV プロテアーゼ阻害剤
ヒドロキシル基を含む基質遷状態アナログが組み込まれている.

ことから薬剤耐性 HIV に有用であると期待できる. わが国でも，玉村らによるペプチド性 CXCR4 結合阻害剤の研究が精力的に進められ，有用なリード化合物が得られている[4].

一方，インテグラーゼ阻害剤はウイルス DNA を宿主細胞に取り込む段階を阻害するもので，臨床試験中のものがいくつかある. そのほか, HIV プロテアーゼによる切断後の gag プロセシングの最終段階であるカプシドタンパク質 p25 が p24 への変換を阻害するマチュレーション阻害剤についても，臨床試験まで進んでいる.

HIV プロテアーゼ阻害剤

HAART の普及は HIV プロテアーゼ阻害剤の導入が大きく貢献している. 99 個のアミノ酸残基からなる HIV プロテアーゼは，その配列の 25 ～ 27 位にアスパラギン酸プロテアーゼ活性中心に特徴的な Asp-Thr-Gly 配列をもち，ホモダイマーを形成することで活性を発現している. 酵素活性中心の二つの Asp 残基の触媒作用により，テトラヘドラルな遷移状態を経て基質ペプチド結合を切断する.

この遷移状態を模倣した分子を用いて，活性中心の Asp 残基と安定な非共有結合型の複合体を形成させて酵素活性を阻害する考えが提案された. この概念は当初，血圧調節に関与するレニンや消化酵素のペプシンなどの遷移状態アナログとして阻害剤研究に検討された. その後，そこで得られた経験と知識が総動員され，副作用のないエイズ治療薬を目指した HIV プロテアーゼ阻害剤の開発が着手されたのである. とくに，レトロウイルスプロテアーゼに特徴的な Phe-Pro 基質切断部位に着目することにより，高い選択性をもち，副作用の少ない薬剤の創製が可能になると考えられ，多くの研究機関で精力的な開発が行われた.

現在，サキナビル (商品名：インビラーゼ，フォートベース) は HIV プロテアーゼの三次構造からデザインされた最初の阻害剤として，アメリカ食品医薬品局 (FDA) の承認を受けた. 本剤に使われている基質遷移状態アナログ (ヒドロキシエチルアミン) ではさらに構造活性相関研究が行われ，第 3, 4, 5 番目の HIV プロテアーゼ阻害剤としてインディナビル (商品名：クリキシバン)，ネルフィナビル (商品名：ビラセプト) およびアンプレナビル (商品名：プローゼ) が承認されている.

一方, HIV プロテアーゼの活性体が C2 対称 2 量体であることに着目して開発されたのが，第 2 番目の阻害剤として承認されたリトナビル (商品名：ノービア) である. この薬剤
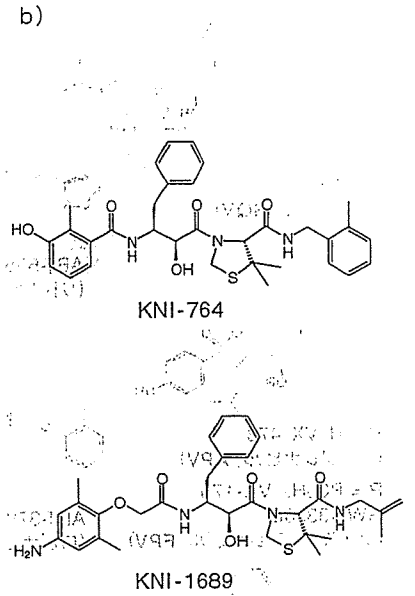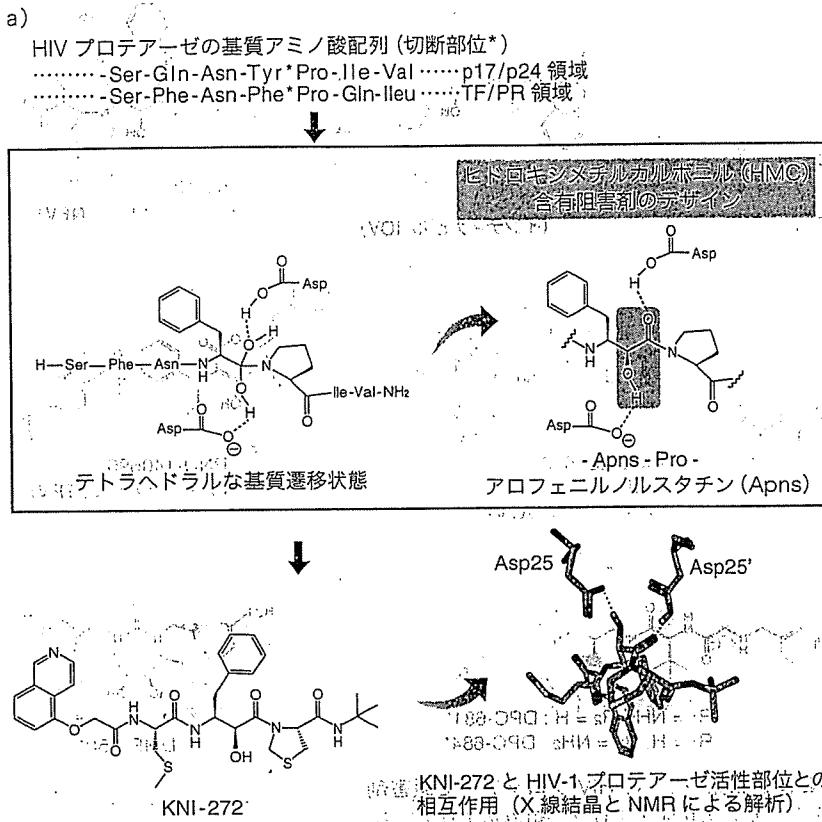
a)

HIV プロテアーゼの基質アミノ酸配列（切断部位*）
............-Ser-Gln-Asn-Tyr*Pro-Ile-Val ......p17/p24 領域
............-Ser-Phe-Asn-Phe*Pro-Gln-Ileu ......TF/PR 領域

ヒドロキシメチルカルボニル（HMC）
含有阻害剤のデザイン

テトラヘドラルな基質遷移状態

- Apns - Pro -
アロフェニルノルスタチン（Apns）

KNI-272

Asp25   Asp25'

KNI-272 と HIV-1 プロテアーゼ活性部位との
相互作用（X線結晶と NMR による解析）

b)

KNI-764

KNI-1689

図4　筆者らが開発した HIV プロテアーゼ
阻害剤
a）KNI-272 開発に至る経緯，b）KNI-272 か
ら改良された同阻害剤．

は肝代謝酵素チトクローム C450 の阻害作用があるため血中半減期が長いので，ほかのプロテアーゼ阻害剤の血中濃度維持のために少量併用される（この手法をブーストという）．

第6番目に承認されたカレトラ（商品名）はロピナビルとリトナビルの配合剤で，耐性ウイルスを生じにくいロピナビルの効果をリトナビルの併用により飛躍的に持続できる特徴がある．第7番目に承認されたアタザナビル（商品名：レイアタッツ）は血中濃度の持続性が高く，1日1回の服用でよいはじめての HIV プロテアーゼ阻害剤である．交差耐性が生じにくく，かつ血中トリグリセリドやコレステロールの上昇といったプロテアーゼ阻害剤特有の副作用がない点が特徴である．

アメリカでは 2005 年6月，第9番目の阻害剤となるティプラナビル（商品名：アプティバス）が承認された．ティプラナビルはライブラリースクリーニングで得られた化合物をもとに開発されたことから，これまでの化合物とは異なる非ペプチド型構造をしている．耐性 HIV に高い効力をもつため，今後の活用が期待される．

次に FDA の承認を待ち構えるのは TMC-114[5]で，bis-THF を保有することでプロテアーゼと非常に高い親和性があり，耐性 HIV にも強力な活性を維持する．現在，第Ⅲ相

の臨床試験中である．

ティプラナビルや TMC-114 は，リトナビルをブーストして用いることで，血中濃度持続性の問題をクリアしているほか，DPC-681 や DPC-684[6]も耐性株に高活性をもつものとして医薬品候補化合物質として開発されており，その効果が期待されている．また，DMP-450[7]のような分子モデリングを駆使した de novo デザインも精力的に研究されている．

筆者らも，1989 年に HIV プロテアーゼを標的とした抗エイズ薬の開発研究に着手し，酵素の加水分解における基質遷移状態を考慮した化合物のデザイン，構造活性相関研究を展開した．その結果，基質遷移状態誘導体として，HIV プロテアーゼの基質ペプチド配列の Phe-Pro ペプチド結合にヒドロキシメチルカルボニル（HMC）構造をもつ Apns（アロフェニルノルスタチン）を母核とした化合物が合成され，強力かつ特異的な HIV プロテアーゼ阻害作用をもつトリペプチド誘導体，KNI-272 が見いだされた（図 4a）[8]．

KNI-272 が，V32I/L33F/K45I/F53L/A71V/I84V という変異株において活性を 130 分の1に低下させたことを受け，酵素・阻害剤複合体の分子レベルでの詳細な研究を通し，Apns 含有化合物のさらなる構造活性相関研究を進めた

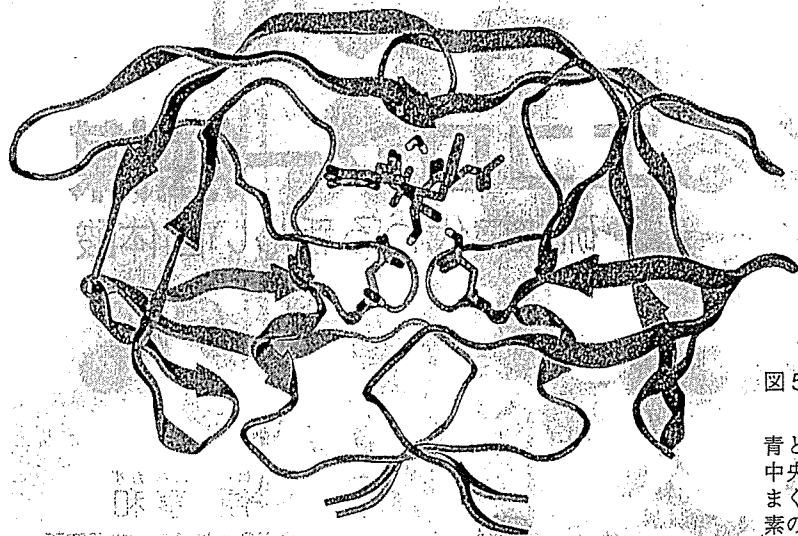図5 HIV-1 プロテアーゼに結合する KNI-1689 のX線結晶構造
青と赤のリボンは HIV-1 プロテアーゼのホモダイマー。中央の緑は KNI-1689 を示す。二つの Asp と HMC はうまく相互作用しており，KNI-1689 は水1分子を介して酵素のフラップ部分（上部）と結合している。

結果，耐性株にも有効なジペプチド型阻害剤 KNI-764（別名：JE-2147，AG-1776，SM-319777）の開発に成功した（図4b）。KNI-764 のフェノール性ヒドロキシル基はグルクロン酸縫合を受けることから，薬物動態が改善された SM-322377 へと改良されている[9]。

最近，筆者らは KNI-764 よりも優れた抗 HIV 活性をもつ新規化合物 KNI-1689 を得ることに成功し（図4b）[10]，現在は HIV-1 プロテアーゼとの複合体のX線結晶構造解析の結果（図5）をもとに研究を続けている。また，HMC を含有する擬似対称型阻害剤も検討している[11]。

プロテアーゼ阻害剤を大量に投与すると，肝臓，腎臓への負荷や，嘔吐，下痢など消化器系をはじめとする副作用が発生するなどの問題が知られている。さらに，プロテアーゼ阻害剤は疎水性の酵素活性中心と良好に結合するため高脂溶性を示して水に溶けにくく，経口吸収性に改善の余地がある。第8番目の承認薬フォスアンプレナビル（商品名：レクシヴァ）は，アンプレナビルのヒドロキシル基をリン酸化し，水溶性を改善したプロドラッグである。溶解補助剤を使わない分，1錠中の薬剤量を減らすことができ，服用率の改善が期待できる。筆者らも，ペプチド化学反応を基盤とし，化学的に阻害剤を再生できる新規水溶性プロドラッグを開発し，水溶性と経口吸収性の改善に成功している[12]。

このほか筆者らは，HIV プロテアーゼ阻害剤と逆転写酵素阻害剤とを共有結合により一分子化する新しい概念「ダブルドラッグ」の提唱[13]のほか，HIV プロテアーゼの二量体形成を阻害する化合物の検討も行っている[14]。これらのアプローチはいまだ臨床応用されていないものの，将来のエイズ克服に多大な貢献をもたらすであろう。

治療薬研究全体への波及効果

利便性のよい新たな抗 HIV 薬が次つぎと認可され，今やエイズは慢性疾患に近づきつつあるといわれている。しかし，HIV は根治しないので今後も耐性や副作用の克服を目指した抗 HIV 薬研究が重要でありつづける。

また，この抗 HIV 薬研究は HIV という病気の枠を超え，治療薬研究全体にも大きな波及効果を及ぼしつつある。たとえば HIV プロテアーゼ阻害剤を一例にあげると，分子レベルで理論的に阻害剤をデザイン開発する手法は現在，マラリアやアルツハイマー病の治療薬開発へと応用されている[15,16]。筆者らは現在，さまざまな難病の病原性に重要な役割を果たす生体タンパク質分子に着目し，伝承薬物からプロテオームまでの広範囲の分子認識を基盤とした方法論の確立を目指して，統合創薬科学を展開している[17,18]。このように，今さかんに行われている抗 HIV 研究が今後，別の多様な感染症や疾患の治療薬研究にもおおいに貢献していくものと確信する。

参考文献
1) http://www.aidsinfo.nih.gov/ 2) HIV 感染症「治療の手引き」第9版 (http://www.hivjp.org/). 3) 岡慎一，医学のあゆみ，213, 859 (2005). 4) H. Tamamura et al., Expert Opin. Ther. Targets, 9, 1267 (2005). 5) Y. Koh et al., Antimicrob. Agents Chemother., 47, 3123 (2003). 6) D. P. Getman et al., U.S. Patent 6172101 (2001). 7) G. V. De Lucca et al., Pharm. Biotechnol., 11, 257 (1998). 8) Y. Kiso, Biopolymers, 40, 235 (1996). 9) T. Mimoto et al., Bioorg. Med. Chem., 12, 281 (2004). 10) H. M. Abdel-Rahman et al., Arch. Pharm. Pharm. Med. Chem., 337, 587 (2004). 11) K. Hidaka et al., Bioorg. Med. Chem. Lett., 13, 93 (2003). 12) Y. Sohma et al., J. Med. Chem., 46, 4124 (2003). 13) H. Matsumoto et al., Bioorg. Med. Chem., 9, 1589 (2001). 14) M. S. Song et al., Bioorg. Med. Chem. Lett., 11, 2465 (2001). 15) Science, 301, 143 (2003), editors' choice. 16) M. Asai et al., J. Neurochem., 96, 533 (2006). 17) 木曽良明，林良雄，日高興士，MEDCHEM NEWS, 15, 11 (2005). 18) 木曽良明，BIO Clinica, 21, 16 (2006).

β-Secretase inhibitors: Modification at the P4 position and improvement of inhibitory activity in cultured cells

Yoshio Hamada,[a] Naoto Igawa,[a] Hayato Ikari,[a] Zyta Ziora,[a] Jeffrey-Tri Nguyen,[a] Abdellah Yamani,[a] Koushi Hidaka,[a] Tooru Kimura,[a] Kazuki Saito,[b] Yoshio Hayashi,[a] Maiko Ebina,[c] Shoichi Ishiura[c] and Yoshiaki Kiso[a],*

[a]Department of Medicinal Chemistry, Center for Frontier Research in Medicinal Science and 21st Century COE Program, Kyoto Pharmaceutical University, Yamashina-ku, Kyoto 607-8412, Japan
[b]Laboratory of Proteomic Sciences, 21st Century COE Program, Kyoto Pharmaceutical University, Yamashina-ku, Kyoto 607-8412, Japan
[c]Department of Life Sciences, Graduate School of Arts and Sciences, University of Tokyo, Meguro-ku, Tokyo 153-8902, Japan

Abstract—Recently, we reported potent and small-sized β-secretase (BACE1) inhibitors KMI-570 and KMI-684 in which we replaced carboxylic acid groups at the P_1' position of KMI-420 and KMI-429, respectively, with tetrazole derivatives as carboxylic acid bioisosteres. These modifications improved significantly BACE1 inhibitory activity and chemical stability. In this study, the acidic tetrazole ring of the P_4 position of KMI-420 and KMI-570, respectively, was replaced with various hydrogen bond acceptor groups. We found BACE1 inhibitor KMI-574 that exhibited potent inhibitory activity in cultured cells as well as in vitro enzymatic assay.
© 2006 Elsevier Ltd. All rights reserved.

According to the amyloid hypothesis,[1] β-secretase [BACE1: β-site APP (amyloid precursor protein) cleaving enzyme] is a molecular target for therapeutic intervention in Alzheimer's disease (AD),[2–6] because BACE1 triggers amyloid β (Aβ) peptide formation by cleaving APP at the N-terminus of the Aβ domain.[7–12] Recently, we reported small-sized BACE1 inhibitors KMI-420 (1) and KMI-429 (2),[13] that contained phenylnorstatine [Pns: (2R,3S)-3-amino-2-hydroxy-4-phenylbutyric acid] as a substrate transition-state mimic.[14] KMI-429 exhibited effective inhibition of BACE1 activity in cultured cells, and significant reduction of Aβ production in vivo (APP transgenic and wild-type mice).[13b] Furthermore, KMI-570 (3) and KMI-684 (4), in which the carboxylic acids at the P_1' position of KMI-420 and KMI-429, respectively, were replaced with tetrazole rings, showed more potent BACE1 inhibitory activity[15] (Fig. 1). According to structure–activity relationship
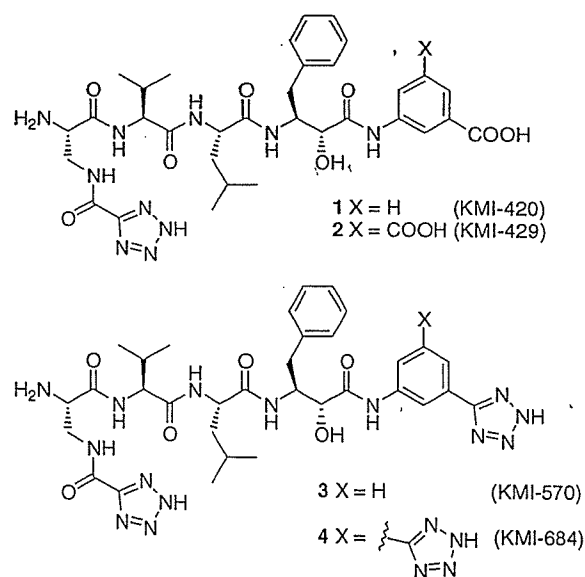

Figure 1. Structures of BACE1 inhibitors containing a tetrazole ring at the P_4 position.

studies of KMI-compounds, an acidic moiety at the P_4 position is required for improving BACE1 inhibitory activity. Moreover, according to substrate specificity[16] and crystal structure[17] studies of BACE2, an acidic moiety at the P_4 position is thought to be important for selectivity against BACE2. Inhibition of BACE2, a homologue enzyme of BACE1,[18,19] by nonselective BACE1 inhibitors may compromise the desired decrease of Aβ, because BACE2 has been reported to regulate Aβ formation as well as α-secretase as an indirect antagonist of BACE1.[20,21] Hence, the presence of an acidic moiety or hydrogen bond acceptor at the P_4 position of BACE1 inhibitors would improve selectivity over BACE2, because of favored interactions with Arg307 in the S_4 pocket of BACE1 over the corresponding Gln in BACE2.[17] However, acidic moieties often possess low membrane permeability across the blood–brain barrier. In this paper, we replaced the respective acidic tetrazole ring at the P_4 position of KMI-420 and KMI-570 with other hydrogen bond acceptor groups and evaluated BACE1 inhibitory activity in cultured cells (BACE1-transfected HEK293 cells) in order to develop practical anti-Alzheimer's disease drugs. By replacing with a 5-fluoroorotyl group at the P_4 position and L-cyclohexylalanine (Cha) residue at the P_2 position likewise, we found BACE1 inhibitor KMI-574 that showed potent BACE1 inhibitory activity in cultured cells as well as in vitro enszymatic assay.

BACE1 inhibitors 5–22 were synthesized by Fmoc-based (9-fluorenylmethoxycarbonyl) solid-phase peptide synthesis methods according to previously reported procedures.[13a] As examples, the syntheses of inhibitors 16 and 22 are outlined in Scheme 1. Briefly, N-Fmoc-3-aminobenzoic acid or N-Fmoc-5-(3-aminophenyl)tetrazole was attached to 2-chlorotrityl chloride resin using diisopropylethylamine (DIPEA) in dichloromethane (DCM). The Fmoc group was removed with 20% piperidine in DMF and peptide bonds were formed using diisopropylcarbodiimide (DIPCDI) as coupling reagent in the presence of 1-hydroxybenzotriazole (HOBt). After elongating the peptide chain, cleavage from the resin was achieved using trifluoroacetic acid (TFA) in the presence of m-cresol and thioanisole. The crude peptide was purified by preparative RP-HPLC.

BACE1 inhibitory activity of the inhibitors was determined by enzymatic assay using a recombinant human BACE1 and FRET (fluorescence resonance energy transfer) substrate as previously reported.[5] After the enzymatic reaction with BACE1 and FRET substrate, (7-methoxycoumarin-4-yl)acetyl-Ser-Glu-Val-Asn-Leu*Asp-Ala-Glu-Phe-Arg-Lys(2,4-dinitrophenyl)-Arg-Arg-NH$_2$, in incubation buffer with 2 or 0.2 μM KMI-compounds, the N-terminal cleavage fragment of the substrate was analyzed by RP-HPLC with fluorescence detection. BACE1 inhibitory activity in cultured cells was determined in the manner reported by Asai.[13b] HEK293 cells that stably expressed human BACE1 enzyme (BACE1-HEK293) were cultured in 60 mm dishes until 80–100% confluent (37 °C, 5% CO$_2$ incubator). After replacement by new serum-free medium with or without KMI-compounds (100 μM), BACE1-HEK293
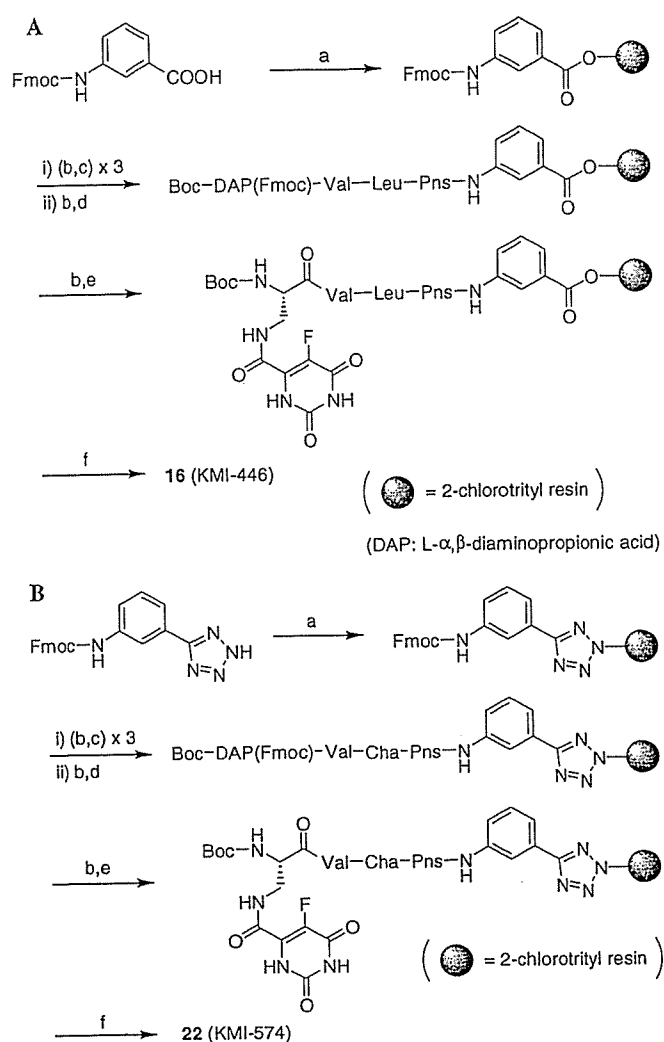
Scheme 1. Reagents: (a) 2-Chlorotrityl chloride resin, DIPEA, DCM; (b) 20% piperidine/DMF; (c) Fmoc-AA-OH, DIPCDI, HOBt, DMF; (d) Boc-DAP(Fmoc)-OH, DIPCDI, HOBt, DMF; (e) 5-fluoroorotic acid, DIPCDI, HOBt, DMF; (f) TFA, m-cresol, thioanisole.

cells were further incubated for 6 h. After precipitating the protein fraction by treatment with trichloroacetic acid, the fraction was mixed with sample buffer containing 2-mercaptoethanol and subjected to 10% SDS-PAGE. To detect sAPPβ (soluble APPβ: N-terminus domain that is released from APP by cleaving at the β-site by BACE1), Western blotting using anti-sAPPβ polyclonal antibody was performed. According to the fluorescence imaging of the bands on the blotting membranes, the amount of sAPPβ peptide, assumed to be the index of BACE1 activity, was measured. BACE1 inhibitory activity in cultured cells was determined by calculating the decrease rate of sAPPβ levels against the control using DMSO instead of KMI-compounds solution.

We selected inhibitor 1 (KMI-420), possessing a carboxylic acid at the P_1' benzene ring, as a parent compound and replaced its tetrazole ring at the P_4 position with various functional groups. The BACE1 inhibitory activity of compounds 5–17 is summarized in Table 1. Inhibitors 6–10 and 15–17, in particular 9 and 16, that contain

Table 1. Effects of P$_4$ modification on BACE1 inhibitory activity of KMI-420
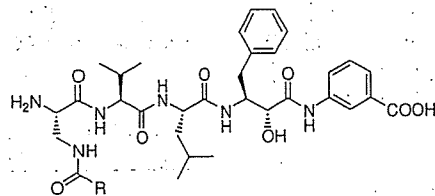
Compound (KMI No.)	R	BACE1 inhibition (%)		BACE1 inhibition (%) in cultured cells at 100 μM
		at 2 μM	at 0.2 μM	
5 (KMI-471)		75	—	29
6 (KMI-479)		91	49	57
7 (KMI-520)		89	75	~0
8 (KMI-521)		86	59	20
9 (KMI-522)		98	84	58
10 (KMI-473)		94	60	69
11 (KMI-523)		82	38	4
12 (KMI-468)		69	—	—
13 (KMI-508)		40	—	—
14 (KMI-509)		13	—	—
15 (KMI-467)		90	54	46
16 (KMI-446)		99	82	76
17 (KMI-510)		99	72	73
1 (KMI-420)		99	87	—
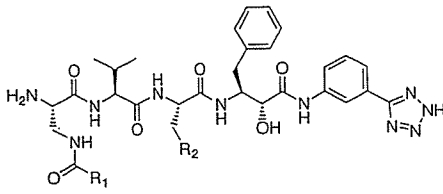
aromatic hydrogen bond acceptors at the P$_4$ position showed potent BACE1 inhibitory activity by *in vitro* enzymatic assay. In cultured cells, inhibitors 16 and 17 possessing ureide derivatives at the P$_4$ position exhibited higher BACE1 inhibitory activities in cultured cells than inhibitors 5–11 and 15.
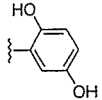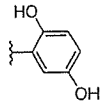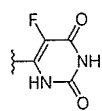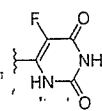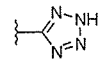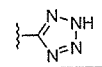
Replacing the Leu residue at the P$_2$ position with the unnatural amino acid Cha slightly enhanced BACE1 inhibitory activity (18 cf. 3, Table 2). Peptides containing unnatural amino acids are expected to possess improved stability *in vivo*. Using 2,5-dihydroxybenzoyl or 5-fluoro-orotyl groups, corresponding inhibitors 9 and 16 at the P$_4$ position and Leu or Cha residues at the P$_2$ position, we synthesized inhibitors 19–22 that contain a tetrazole ring on the P$_1$' benzene ring. As shown in Table 2, inhibitors 19–22 exhibited potent BACE1 inhibitory activity by *in vitro* enzymatic assay that is similar to reference compounds 3 (KMI-570) and 18 (KMI-571). In cultured cells, compound 22 containing a P$_4$ 5-fluoroorotyl group and P$_2$ Cha residue showed potent BACE1 activity, while compound 21 containing a P$_2$ Val residue and compounds 19 and 20 containing P$_4$ phenol derivatives showed moderate inhibitory activity. The difference in BACE1 inhibitory activity between *in vitro* enzymatic and

cultured cell-based assay is thought to be dependent on the cell membrane permeability of the inhibitor. Because endogenous BACE1 is localized predominantly in the later Golgi and *trans*-Golgi network,[22,23] and thought to cleave at the β-site of APP on the *trans*-Golgi network mainly,[23] the synergistic effect of inherent BACE1 inhibitory activity by *in vitro* enzymatic assay and its cell permeability is believed to reflect BACE1 inhibitory activity in cultured cells.

Inhibitors 21 and 22 with 5-fluoroorotyl group at the P$_4$ position exhibited potent BACE1 inhibitory activity by *in vitro* enzymatic assay that is almost similar to that of inhibitor 3 with a tetrazole ring at the same position. Orotyl derivatives, although not classified as bioisosteres for carboxylic acid, and tetrazole rings play a role in enhancing BACE1 inhibitory activity. In order to find structure-based explanations, computational docking simulations were performed using available coordinates for BACE1 (PDB ID: 1W51), using previously reported methods.[13a] The structure of inhibitor 22 docked in BACE1, and that of superimposed previously reported inhibitor 4, which possesses tetrazole rings at the P$_4$ and P$_1$' positions, are shown in Figure 2. In docking experiments, 5-fluoroorotyl and tetrazole-5-carbonyl

Table 2. Effects of P$_4$ modification on BACE1 inhibitory activity of KMI-570 and KMI-571

Compound (KMI No.)	R$_1$	R$_2$	BACE1 inhibition (%)		IC$_{50}$[a] (nM)	BACE1 inhibition (%) in cultured cells at 100 μM
			at 2 μM	at 0.2 μM		
19 (KMI-573)			99	93	—	65
20 (KMI-575)			99	92	—	69
21 (KMI-572)			100	98	6.5	63
22 (KMI-574)			100	97	5.6	84
3 (KMI-570)			100	98	4.8	66
18 (KMI-571)			100	98	3.3	59

[a] IC$_{50}$ values in *in vitro* enzymatic assay.

4358

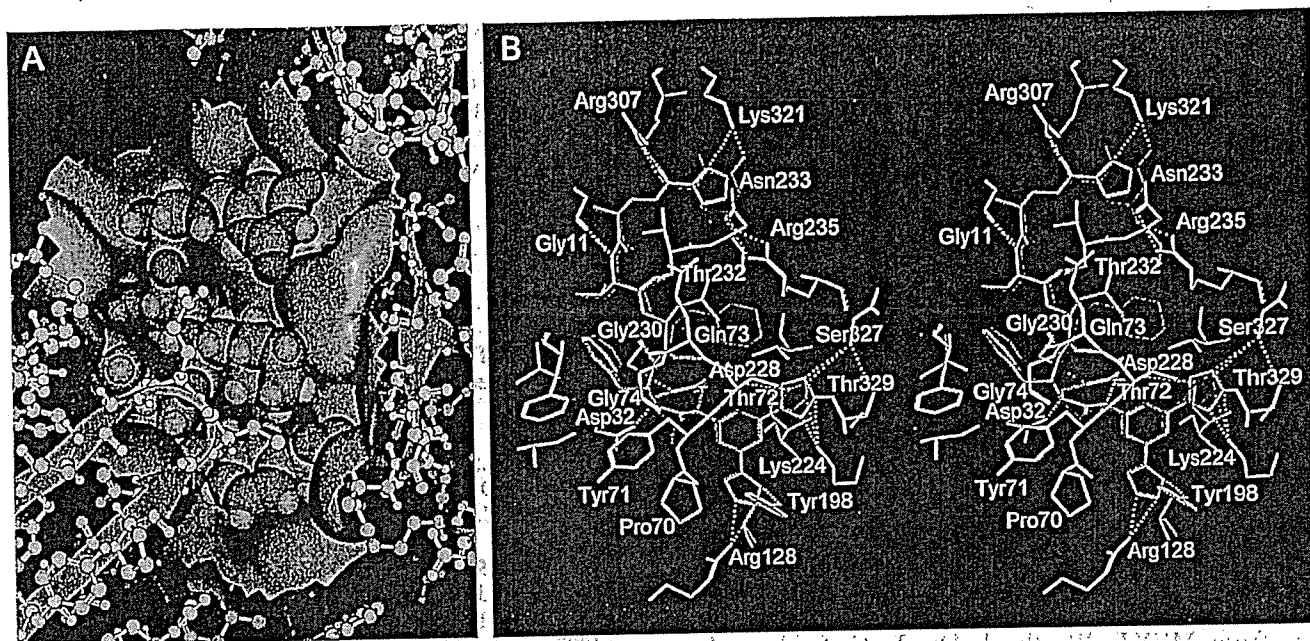*Y. Hamada et al. / Bioorg. Med. Chem. Lett. 16 (2006) 4354–4359*

Figure 2. Docked inhibitor 22 (KMI-574) in BACE1 enzyme (PDB ID: 1W51). (A) Overview of docked inhibitor 22 (space-filling model) in the binding site of BACE1 enzyme. Yellow ball-and-stick and colored molecular-surface models indicate BACE1 and its binding site except for the flap domain from Pro70 to Gly74, respectively. (B) Stereoscopic view of superimposed inhibitors 22 (red lines) and 4 (KMI-684, green lines). Yellow and white dashed lines indicate BACE1 enzyme and hydrogen bond interactions, respectively.

groups each assumed the same pose in the binding pocket of BACE1 that consists of Arg307, Lys321, and Arg235, whereas the former group is larger than the latter. On the other hand, inhibitor 16, which contained a fluorine atom on the aromatic ring, showed higher BACE1 inhibitory activity than inhibitors 15 and 17. The strong electron-withdrawing fluorine atom raises the electrophilicity of the aromatic ring, consequently enhancing the hydrogen bond acceptor character of the P_4 side chain. This effect is likely to improve BACE1 inhibitory activity.

High affinity for the BACE1 enzyme does not necessitate high BACE1 inhibition in cultured cells because of various factors affecting cellular penetration. Bhhatarai and Garg have used calculated log P (Clog$P$) and calculated molar refractivity (CMR) values to predict the inhibitory activity of HIV-1 protease inhibitors.[24] (k_1 Clog$P$–k_2 ClogP^2) can be seen as the inhibitor's lipophilicity value, while (k_3 CMR–k_4 CMR^2) represents the inhibitor's steric effect, that both would favor internalization of the inhibitor into the cell. The following QSAR equation, derived from compounds 3, 8, 9, 11, and 15–22, was obtained with a high regression fit ($r^2 = 0.933$) and significance ($p < 0.001$) when inhibitors 6, 7, and 10 were excluded as outliers by cross-validation.

$$\log(\text{Inh}_{cell}) = 1.889 \log(\text{Inh}_{enz}) - (0.169 \text{Clog} P)$$
$$- 0.042 k_1 \text{Clog} P^2) - (4.351 \text{CMR}$$
$$- 0.104 \text{CMR}^2) - 45.666 \qquad (1)$$

$$n = 12, \quad r^2 = 0.933, \quad F = 16.679, \quad p < 0.001$$

Inh$_{cell}$ denotes percent BACE1 inhibition with 100 µM in cultured cells, while Inh$_{enz}$ denotes percent BACE1

inhibition with 0.2 µM inhibitor by enzymatic assay. Clog$P$ and CMR values were calculated with ChemDraw Ultra 6, while statistical evaluations were performed in Microsoft Excel 2003.

The QSAR equation predicts that an inhibitor with Clog$P$ of less than −1.006 and CMR of 21.080 would exhibit potent cellular activity. It should be noted that an inhibitor with a low Clog$P$ value may have a detrimental CMR value, because relationships exist between Clog$P$ and CMR. Calculations also reveal that the inhibitor's intrinsic activity (Inh$_{enz}$) is the major determinant, while Clog$P$ is a lesser determinant for cellular inhibitory activity than CMR, suggesting that CMR is a more accurate predictor than Clog$P$. Although the results obtained from the equation are rough estimates (Fig. 3), the QSAR equation is invaluable to design BACE1 inhibitors with high cellular activity, especially when the QSAR equation
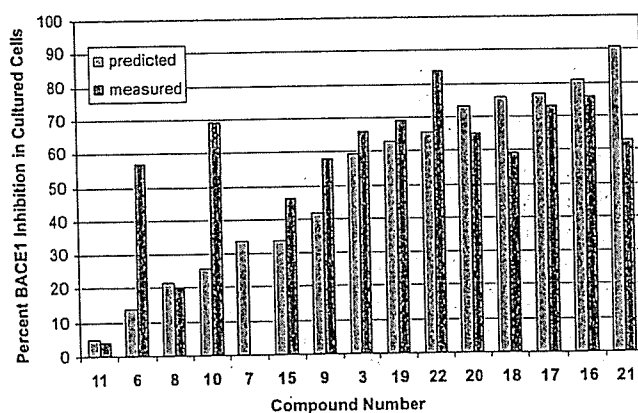

Figure 3. Predicted BACE1 inhibitory activities in cultured cells using multiple linear regression by Eq. 1 and their observed values for inhibitors 3, 6–11, and 15–22.

is further refined as more cellular BACE1 inhibition data become available in future research.

In conclusion, BACE1 inhibitors were designed and synthesized using various hydrogen bond acceptor groups at the P_4 position and Cha residue replacement at the P_2 position. BACE1 inhibitor 22 (KMI-574) exhibited potent BACE1 inhibitory activity in cultured cells as well as *in vitro* enzymatic assay. These findings are a stepping stone forward to overcome a key issue in developing of anti-AD drugs, namely to improve cell and blood–brain barrier permeability.

References and notes

1. (a) Hong, L.; Koelsch, G.; Lin, X.; Wu, S.; Terzyan, S.; Ghosh, A. K.; Zhang, X. C.; Tang, J. *Science* 2000, *290*, 150; (b) Sipe, J. D. *Annu. Rev. Biochem.* 1992, *61*, 947; (c) Selkoe, D. J. *Ann. N.Y. Acad. Sci.* 2000, *924*, 17; (d) Steiner, H.; Capell, A.; Leimer, U.; Haass, C. *Eur. Arch. Psychiatric. Clin. Neurosci.* 1999, *249*, 266; (e) Selkoe, D. J. *Ann. Med.* 1989, *21*, 73.
2. (a) Ghosh, A. K.; Shin, D.; Downs, D.; Koelsch, G.; Lin, X.; Ermolieff, J.; Tang, J. *J. Am. Chem. Soc.* 2000, *122*, 3522; (b) Ghosh, A. K.; Bilcer, G.; Harwood, C.; Kawahara, R.; Shin, D.; Hussain, K. A.; Hong, L.; Loy, J. A.; Nguyen, C.; Koelsch, G.; Ermolieff, J.; Tang, J. *J. Med. Chem.* 2001, *44*, 2865.
3. Tung, J. S.; Davis, D. L.; Anderson, J. P.; Walker, D. E.; Mamo, S.; Jewett, N.; Hom, R. K.; Sinha, S.; Thorsett, E. D.; John, V. *J. Med. Chem.* 2002, *45*, 259.
4. Tamamura, H.; Kato, T.; Otaka, A.; Fujii, N. *Org. Biomol. Chem.* 2003, *1*, 2468.
5. Shuto, D.; Kasai, S.; Kimura, T.; Liu, P.; Hidaka, K.; Hamada, T.; Shibakawa, S.; Hayashi, Y.; Hattori, C.; Szabo, B.; Ishiura, S.; Kiso, Y. *Bioorg. Med. Chem. Lett.* 2003, *13*, 4273.
6. (a) Kimura, T.; Shuto, D.; Kasai, S.; Liu, P.; Hidaka, K.; Hamada, T.; Hayashi, Y.; Hattori, C.; Asai, M.; Kitazume, S.; Saido, T. C.; Ishiura, S.; Kiso, Y. *Bioorg. Med. Chem. Lett.* 2004, *14*, 1527; (b) Ziora, Z.; Kimura, T.; Kiso, Y. *Drugs Future* 2006, *31*, 53.
7. Vassar, R.; Bennett, B. D.; Babu-Khan, S.; Kahn, S.; Mendiaz, E. A.; Denis, P.; Teplow, D. B.; Ross, S.; Amarante, P.; Loeloff, R.; Luo, Y.; Fisher, S.; Fuller, J.;

8. Edenson, S.; Lile, J.; Jarosinski, M. A.; Biere, A. L.; Curran, E.; Burgess, T.; Louis, J. C.; Collins, F.; Treanor, J.; Rogers, G.; Citron, M. *Science* 1999, *286*, 735.
8. Yan, R.; Bienkowski, M. J.; Shuck, M. E.; Miao, H.; Tory, M. C.; Pauley, A. M.; Brashier, J. R.; Stratman, N. C.; Mathews, W. R.; Buhl, A. E.; Carter, D. B.; Tomasselli, A. G.; Parodi, L. A.; Heinrikson, R. L.; Gurney, M. E. *Nature* 1999, *402*, 533.
9. Sinha, S.; Anderson, J. P.; Barbour, R.; Basi, G. S.; Caccavello, R.; Davis, D.; Doan, M.; Dovey, H. F.; Frigon, N.; Hong, J.; Jacobson-Croak, K.; Jewett, N.; Keim, P.; Knops, J.; Lieberburg, I.; Power, M.; Tan, H.; Tatsuno, G.; Tung, J.; Schenk, D.; Seubert, P.; Suomensaari, S. M.; Wang, S.; Walker, D.; Zhao, J.; McConlogue, L.; John, V. *Nature* 1999, *402*, 537.
10. Hussain, I.; Powell, D.; Howlett, D. R.; Tew, D. G.; Meek, T. D.; Chapman, C.; Gloger, I. S.; Murphy, K. E.; Southan, C. D.; Ryan, D. M.; Smith, T. S.; Simmons, D. L.; Walsh, F. S.; Dingwall, C.; Christie, G. *Mol. Cell. Neurosci.* 1999, *14*, 419.
11. Selkoe, D. J. *Nature* 1999, *399*, A23.
12. Sinha, S.; Lieberburg, I. *Proc. Natl. Acad. Sci. U.S.A.* 1999, *96*, 11049.
13. (a) Kimura, T.; Shuto, D.; Hamada, Y.; Igawa, N.; Kasai, S.; Liu, P.; Hidaka, K.; Hamada, T.; Hayashi, Y.; Kiso, Y. *Bioorg. Med. Chem. Lett.* 2005, *15*, 211; (b) Asai, M.; Hattori, C.; Iwata, N.; Saido, T. C.; Sasagawa, N.; Szabó, B.; Hashimoto, Y.; Maruyama, K.; Tanuma, S.; Kiso, Y.; Ishiura, S. *J. Neurochem.* 2006, *96*, 533.
14. (a) Mimoto, T.; Imai, J.; Tanaka, S.; Hattori, N.; Takahashi, O.; Kisanuki, S.; Nagano, Y.; Shintani, M.; Hayashi, H.; Akaji, K.; Kiso, Y. *Chem. Pharm. Bull.* 1991, *39*, 2465; (b) Mimoto, T.; Imai, J.; Tanaka, S.; Hattori, N.; Kisanuki, S.; Akaji, K.; Kiso, Y. *Chem. Pharm. Bull.* 1991, *39*, 3088.
15. Kimura, T.; Hamada, Y.; Stochaj, M.; Ikari, H.; Nagamine, A.; Abdel-Rahman, H.; Igawa, N.; Hidaka, K.; Nguyen, J-T.; Saito, K.; Hayashi, Y.; Kiso, Y. *Bioorg. Med. Chem. Lett.* 2006, *16*, 2380.
16. Farzan, M.; Schnitzler, C. E.; Vasilieva, N.; Leung, D.; Choe, H. *Proc. Natl. Acad. Sci. U.S.A.* 2000, *97*, 9712.
17. Ostermann, N.; Eder, J.; Eidhoff, U.; Zink, F.; Hassiepen, U.; Worpenberg, S.; Maibaum, J.; Simic, O.; Hommel, U.; Gerhartz, B. *J. Mol. Biol.* 2006, *355*, 249.
18. Yan, R.; Bienkowski, M. J.; Shuck, M. E.; Miao, H.; Tory, M. C.; Pauley, A. M. *Nature* 1999, *402*, 533–537.
19. Acquati, F.; Accarino, M.; Nucci, C.; Fumagalli, P.; Jovine, L.; Ottolenghi, S.; Taramelli, R. *FEBS Lett.* 2000, *468*, 59.
20. Basi, G.; Frigon, N.; Barbour, R.; Doan, T.; Gordon, G.; McConlogue, L.; Sinha, S.; Zeller, M. *J. Biol. Chem.* 2003, *278*, 31512.
21. Sun, X.; Wang, Y.; Qing, H.; Christensen, M. A.; Liu, Y.; Zhou, W.; Tong, Y.; Xiao, C.; Huang, Y.; Zhang, S.; Liu, X.; Song, W. *FASEB J.* 2005, *19*, 739.
22. Yan, R.; Han, P.; Miao, H.; Greengard, P.; Xu, H. *J. Biol. Chem.* 2001, *276*, 36788.
23. Huse, J. T.; Liu, K.; Pijak, D. S.; Carlin, D.; Lee, V. M.-Y.; Doms, R. W. *J. Biol. Chem.* 2002, *277*, 16278.
24. Bhhatarai, B.; Garg, R. *Bioorg. Med. Chem. Lett.* 2005, *13*, 4078.

ELSEVIER

Development of first photoresponsive prodrug of paclitaxel

Mariusz Skwarczynski,[a] Mayo Noguchi,[a] Shun Hirota,[b,c]
Youhei Sohma,[a,b] Tooru Kimura,[a] Yoshio Hayashi[a,*] and Yoshiaki Kiso[a,*]

[a]Department of Medicinal Chemistry, Center for Frontier Research in Medicinal Science and 21st Century COE Program,
Kyoto Pharmaceutical University, Yamashina-ku, Kyoto 607-8412, Japan
[b]Department of Physical Chemistry, 21st Century COE Program, Kyoto Pharmaceutical University,
Yamashina-ku, Kyoto 607-8412, Japan
[c]PRESTO, JST, Kawaguchi, Saitama 332-0012, Japan

Abstract—A prodrug of paclitaxel which has a coumarin derivative conjugated to the amino acid moiety of isotaxel (O-acyl isoform of paclitaxel) has been synthesized. The prodrug was selectively converted to isotaxel by visible light irradiation (430 nm) with the cleavage of coumarin. Finally, paclitaxel was released by subsequent spontaneous O–N intramolecular acyl migration.
© 2006 Elsevier Ltd. All rights reserved.

A large number of anticancer agents have been developed in recent decades. However, these agents have very little or no specificity for the target tumor tissues which leads to systemic toxicity. Among them, paclitaxel (1, Taxol®) is considered to be one of the most important drugs in cancer chemotherapy. However, this agent also has low tumor selectivity.

To overcome this problem, prodrug strategy is specially promising.[1,2] A lot of prodrugs of paclitaxel have already been designed to specifically deliver them to the tumor tissues with a site-specific chemical delivery system. In addition, macromolecular prodrugs showed targetable properties due to enhanced permeability and retention (EPR) effect, and monoclonal antibodies (mAbs) were used as a vehicle to deliver 1 selectively to the tumor tissues. Some of them exhibited very promising properties; however, none of them is available in clinical use.[3,4]

Photodynamic therapy (PDT) is used for cancer treatment. This technique is based on the administration of a sensitizer devoid of mutagenic properties, followed by the exposure of the pathological area to visible light.[5] Two types of photoreaction mechanisms are invoked to explain photosensitizer action: free radical generation by electron or proton transfer, or singlet oxygen generation by energy transfer, from light activated photosensitizers. To date, the FDA has approved a photosensitizing agent, porphyrin derivative, called Photofrin® for the use in PDT.[6]

Photoactivation also affords a useful technique in life science to monitor biological processes by using so-called 'caged' compounds.[7–12] These compounds are artificial molecules whose biological activity is masked by a covalently attached photocleavable group which can be selectively removed upon light activation to release parent bioactive molecules. Recently, we applied this caged strategy for a controlled generation of intact amyloid β peptide 1–42 (Aβ1–42) for the study of Alzheimer's disease in combination with an isopeptide method to mask biological features of Aβ1–42. A synthesized phototriggered Aβ1–42 isopeptide ('click peptide') possessing a photocleavable 6-nitroveratryloxycarbonyl (Nvoc) group afforded intact Aβ1–42 with a quick and one-way conversion reaction through photoirradiation by 355 nm light and subsequent spontaneous O–N intramolecular acyl migration reaction.[13]

Taking all those three strategies (prodrug, photodynamic therapy, and caged compound chemistry) into consideration, we designed a photoresponsive targeting prodrug of paclitaxel 1, namely phototaxel 2, which has a coumarin derivative conjugated to an amino group

of isotaxel (3, *O*-acyl isoform of paclitaxel).[14–16] This prodrug was expected to: (a) be selectively activated by visible light irradiation (430 nm) leading to cleavage of coumarin, then (b) release paclitaxel via subsequent spontaneous O–N intramolecular acyl migration reaction (Fig. 1). 7-*N*,*N*-Diethylamino-4-hydroxymethyl coumarin (5, DECM) was chosen as a photolabile group since DECM-caged compounds have been reported to be water-soluble, thermally stable, and rapidly photolyzed by visible light.[9,17,18]

As depicted in Scheme 1, 7-*N*,*N*-diethylamino-4-hydroxymethyl coumarin 5 was prepared from commercially available 7-*N*,*N*-diethylamino-4-methyl coumarin 4 according to the procedure reported by B. Giese and coworkers.[18] Compound 5 was activated by coupling to 4-nitrophenyl chloroformate in presence of DMAP (4-(dimethylamino)pyridine),[12] then allowed to react with 3′-*N*-debenzoylpaclitaxel, which was synthesized by a previously described method,[14,19] to afford 6. Finally, benzoylation of the 2′-hydroxyl group with benzoic acid by the EDC-DMAP method (EDC, 1-ethyl-3-(3-dimethylaminopropyl)carbodiimide), and following HPLC purification with ion-exchange by elution with 12 mM aq HCl gave phototaxel 2 as a HCl salt.[20]
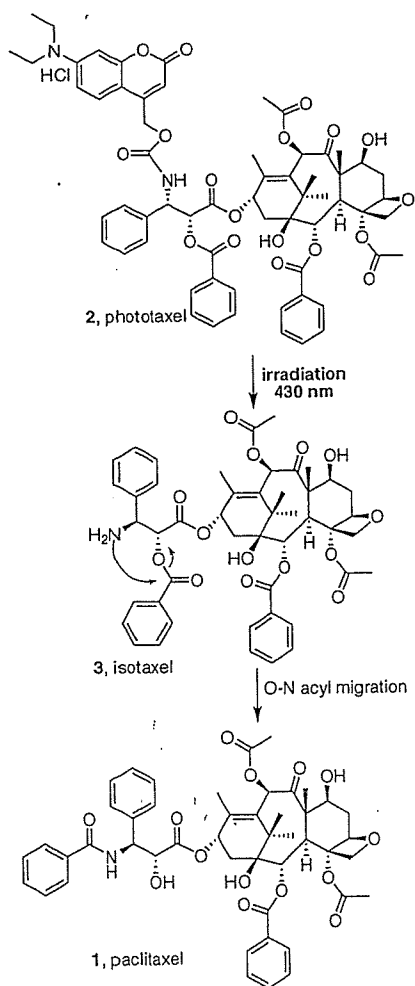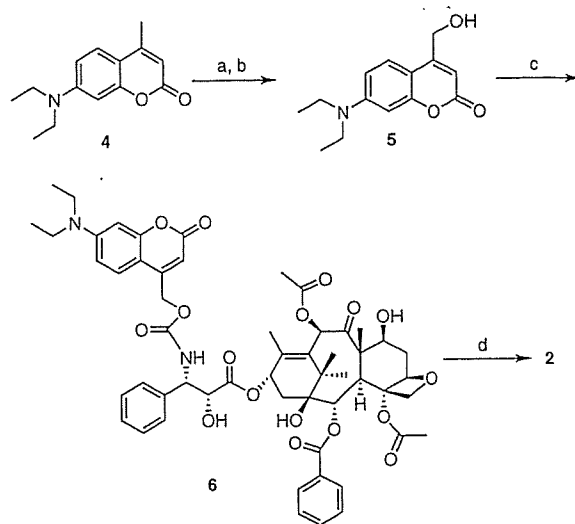

Scheme 1. Syntheses of phototaxel 2. Reagents and conditions: (a) SeO₂, *p*-xylene, reflux, 24 h; (b) NaBH₄, EtOH, rt, 4 h, 49% over two steps; (c) 4-nitrophenyl chloroformate, DMAP, CH₂Cl₂, rt, 6 h, then 3′-*N*-debenzoylpaclitaxel, DMAP, 20 h, 40%; (d) benzoic acid, EDC·HCl, DMAP, CHCl₃, rt, 6 h, then HCl, 70%.

Previously reported DECM-caged compounds demonstrated good water-solubility;[9,17,18] however, prodrug 2 had lower water-solubility (<0.00025 mg mL⁻¹) than parent drug 1. Therefore, to study the kinetics of photoconversion, 2 was dissolved in a mixture of 0.1 M phosphate buffer (PB, pH 7.4) and methanol (1:1, v/v) to simulate physiological conditions[21] and to obtain concentration of prodrug enough high for the clear detection in further evaluations (20–50 μM). Prodrug 2 was photoirradiated with a diode laser (Melles Griot-85 BTL 010 laser, 430.6 nm, 10 mW) at 15 °C. The absorption spectra were taken immediately after irradiation (Fig. 2A). Photolysis of DECM-caged compound is expected to produce compound 5,[9,18] which can be observed as a shift of long-wavelength absorption maximum to the lower wavelength (compounds 5 and 2 had intensive maxima at 385 and 393 nm, respectively). Indeed, we observed not only the shift but also a significant reduction of absorption intensity. This suggested that 2 was photolytically cleaved and the released coumarin derivative was partially decomposed. This observation was further confirmed by HPLC analysis (Fig. 2B), which was performed after irradiation followed by incubation at rt for at least 1 h to induce complete O–N intramolecular acyl migration to the parent paclitaxel (the $t_{1/2}$ value of migration of isotaxel 3 to release 1 was 15.1 min under physiological conditions).[14–16] On the HPLC charts three signals were identified by mass spectrometry analysis and confirmed with independently synthesized compounds as 5 (rt = 20.5 min), 1 (rt = 28.5 min), and 2 (rt = 36.0 min). Thus, time-dependent parent drug release from phototaxel 2 was indicated and quantitative analysis of prodrug kinetics upon photoirradiation (Fig. 3) showed that paclitaxel was released with 69% yield after 30 min; however, only 20% of 5 was recovered. Prodrug 2 was stable in the dark in phosphate-buffered saline (PBS, pH 7.4) at 4 °C for at least 1 month and as a solid state for at least 4 months at −20 °C.

Figure 1. Releasing mechanism of paclitaxel 1 from its photoresponsive prodrug 2.
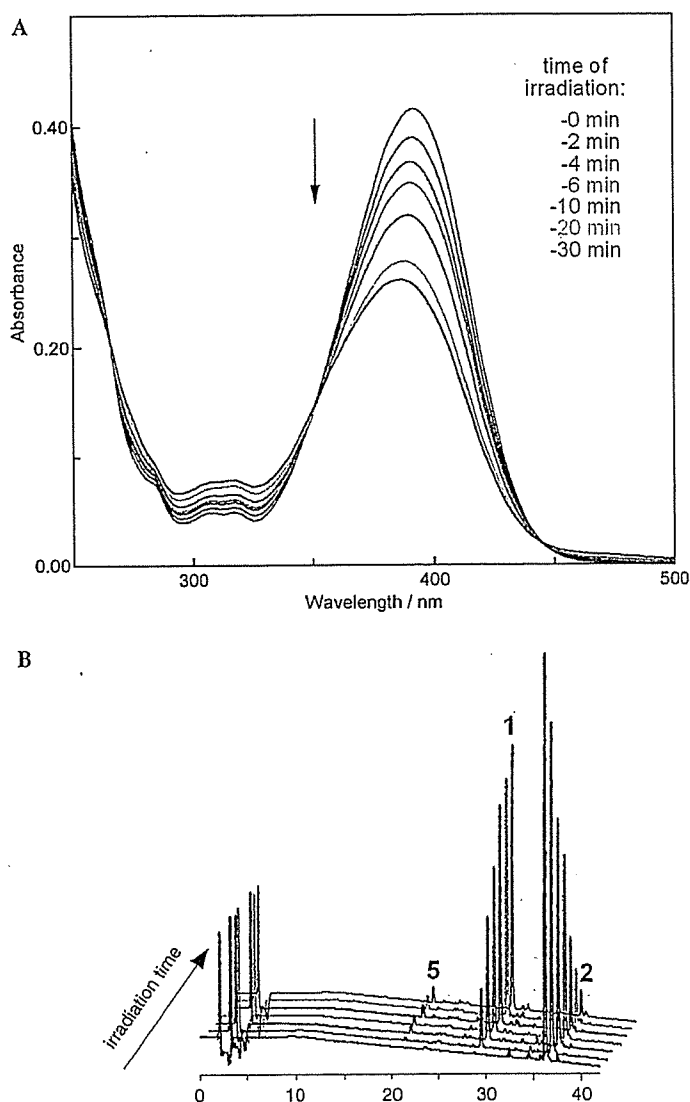
Figure 2. (A) Absorption spectra (250–500 nm) of prodrug 2 solution in PB(0.1 M)/MeOH (1:1) before (red line) and after irradiation (430.6 nm, 10 mW) for desired period of time (other lines) at 15 °C; (B) HPLC charts for prodrug 2 subjected to above irradiation conditions followed by incubation at rt to induce migration, detected at 230 nm (line colors are corresponding to irradiation time in the same manner as for absorption spectra).
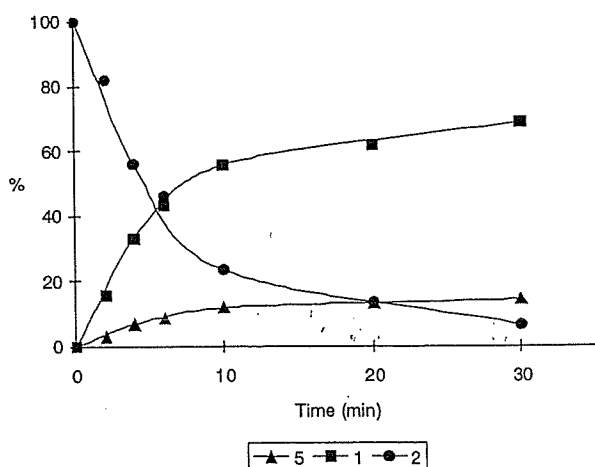

Figure 3. Time course of photolysis of prodrug 2 and release of 5 and 1 in 0.1 M PB/MeOH (1:1) at 430.6 nm. The percentage was determined by HPLC.

Extensive literature searches revealed that photolabile prodrug strategy has not yet been proposed for paclitaxel, although there are a few reports that demonstrated utilization of caged paclitaxel derivatives (activated by UV irradiation) for molecular biology related study.[22,23] Thus, herein a novel approach for developing a photoresponsive tumor targeting paclitaxel prodrug is demonstrated throughout the design and synthesis of phototaxel 2. Prodrug 2 is not expected to be active prior to photoconversion, based on previous SAR studies on paclitaxel derivatives.[24,25] Namely, it is known that both extensive modifications of the N-acyl moiety and masking of the 2′-OH group restrain paclitaxel activity.[25] Upon visible light irradiation (430.6 nm, 10 mW) this prodrug released isotaxel 3 (half-life of prodrug was 4.8 min, Fig. 3), and subsequent spontaneous O–N intramolecular acyl migration ($t_{1/2} = 15.1$ min)[14–16] formed intact paclitaxel 1. This delay of parent drug release after irradiation (related to migration of benzoyl

group) is supposed to be short enough to avoid the intermediate (3) diffusion from the photoirradiated site before the parent drug is released. Moreover, we recently demonstrated faster O–N intramolecular acyl migration in other highly potent taxoids.[14,15,19] For example, prodrug of canadensol (3′-N-isopropylcarbonyl-3′-N-debenzoylpaclitaxel) had a $t_{1/2}$ value of 4.3 min under physiological conditions.[15,19] 2′-O-Benzyloxycarbonyl-3′N-debenzoyl-paclitaxel, prodrug design based on the O–N intramolecular alkoxycarbonyl migration reaction,[26] exhibited even instantaneous conversion to a parent carbamate-type taxoid ($t_{1/2} < 1$ min).[14] Phototaxoids derived from these types of taxoids would be more effective without risking diffusion from the irradiation site.

The observed recovery yield (69%) of paclitaxel 1 in the photo-triggered conversion of 2 in HPLC analysis is in agreement with previous reports on caged compounds (typical released yield was 40–70%).[7,27,28] This relatively moderate recovery might be related to partial decomposition of prodrug 2 or intermediate 3 due to their photoinstability, as we observed low recovery of coumarin derivative 5 from prodrug 2 contrary to a previous report[18] (Figs. 2 and 3). However, no major byproduct formation was detected by HPLC, and paclitaxel 1 was almost stable under the photo-irradiation conditions used for conversion of prodrug 2, that is, only a small amount of paclitaxel decomposition (about 2%) was observed by photo-irradiation for 0.5 h (data not shown). Another reason could be non-specific absorption of compounds on the surface of experimental tubes.

DECM 5 has been chosen as a photolabile group, as much less expensive and simple-to-use light sources are available for experiments in the visible wavelength region. In spite of intensive maxima of DECM-caged compounds are in UV-range (around 390 nm), these compounds have been activated by visible lights (even by irradiation at 436 nm).[9,18] Moreover, during our initial experiments on prodrug 2 irradiated with UV pulses (355 nm, 10 Hz, 5–20 mJ), extensive decomposition of 2 was observed (data not shown). In contrast, irradiation at 430.6 nm showed to be effective for triggering parent drug release without any major decomposition of prodrug or parent drug.

In conclusion, we designed and synthesized a new photoresponsive paclitaxel prodrug based on an idea that combined both photodynamic cancer therapy and caged chemistry. The prodrug, phototaxel 2, released parent drug, paclitaxel, with a reasonable conversion time by visible light irradiation suggesting that this strategy is practically applicable for wide range of anticancer agents to develop new photoresponsive prodrugs. This would expand the current photodynamic therapy which is dependent on photosensitizers (porphyrin derivatives) that generate free radicals or singlet oxygen as cytotoxic spices.

Acknowledgments

References and notes

1. Huang, P. S.; Oliff, A. Curr. Opin. Genet. Dev. 2001, 11, 104.
2. Ferguson, M. J.; Ahmed, F. Y.; Cassidy, J. Drug Resist. Updat. 2001, 4, 225.
3. Jaracz, S.; Chen, Jin.; Kuznetsova, L. V.; Ojima, I. Bioorg. Med. Chem. 2005, 13, 5043.
4. Fang, W.-S.; Liang, X.-T. Mini-Rev. Med. Chem. 2005, 5, 1.
5. MacDonald, I. J.; Dougherty, T. J. J. Porphyrins Phthalocyanines 2001, 5, 105.
6. Vicente, M. G. H. Curr. Med. Chem. Anti-Canc. Agents 2001, 1, 175.
7. Hayashi, K.; Hashimoto, K.; Kusaka, N.; Yamazoe, A.; Fukaki, H.; Tasaka, M.; Nozaki, H. Bioorg. Med. Chem. Lett. 2006, 16, 2470.
8. Zhu, Y.; Pavlos, C. M.; Toscano, J. P.; Dore, T. M. J. Am. Chem. Soc. 2006, 128, 4267.
9. Shembekar, V. R.; Chen, Y.; Carpenter, B. K.; Hess, G. P. Biochemistry 2005, 44, 7107.
10. Wu, N.; Deiters, A.; Cropp, T. A.; King, D.; Schultz, P. G. J. Am. Chem. Soc. 2004, 126, 14306.
11. Hirota, S.; Fujimoto, Y.; Choi, J.; Baden, N.; Katagiri, N.; Akiyama, M.; Hulsker, R.; Ubbink, M.; Okajima, T.; Takabe, T.; Funasaki, N.; Watanabe, Y.; Terazima, M. J. Am. Chem. Soc. 2006, 128, 7551.
12. Furuta, T.; Wang, S. S.-H.; Dantzker, J. L.; Dore, T. M.; Bybee, W. J.; Callaway, E. M.; Denk, W.; Tsien, R. Y. Proc. Natl. Acad. Sci. U.S.A. 1999, 96, 1193.
13. Taniguchi, A.; Sohma, Y.; Kimura, M.; Okada, T.; Ikeda, K.; Hayashi, Y.; Kimura, T.; Hirota, S.; Matsuzaki, K.; Kiso, Y. J. Am. Chem. Soc. 2006, 128, 696.
14. Skwarczynski, M.; Sohma, Y.; Noguchi, M.; Kimura, M.; Hayashi, Y.; Hamada, Y.; Kimura, T.; Kiso, Y. J. Med. Chem. 2005, 48, 2655.
15. Sohma, Y.; Hayashi, Y.; Skwarczynski, M.; Hamada, Y.; Sasaki, M.; Kimura, T.; Kiso, Y. Biopolymers 2004, 76, 344.
16. Hayashi, Y.; Skwarczynski, M.; Hamada, Y.; Sohma, Y.; Kimura, T.; Kiso, Y. J. Med. Chem. 2003, 46, 3782.
17. Geissler, D.; Antonenko, Y. N.; Schmidt, R.; Keller, S.; Krylova, O. O.; Wiesner, B.; Bendig, J.; Pohl, P.; Hagen, V. Angew. Chem. Int. Ed. 2005, 44, 1195.
18. Schonleber, R. O.; Bendig, J.; Hagen, V.; Giese, B. Bioorg. Med. Chem. 2002, 10, 97.
19. Skwarczynski, M.; Sohma, Y.; Kimura, M.; Hayashi, Y.; Kimura, T.; Kiso, Y. Bioorg. Med. Chem. Lett. 2003, 13, 4441.
20. ^{1}H NMR (CDCl$_3$, 400 MHz): δ = 8.03 (d, J = 4.5 Hz, 2H), 7.97 (d, J = 6.6 Hz, 2H), 7.61 (t, J = 6.8 Hz, 1H), 7.52–7.21 (m, 10H), 7.02 (br s, 1H), 6.51–6.38 (m, 3H), 6.30 (s, 1H), 6.00 (br s, 2H), 5.67 (d, J = 7.3 Hz, 1H), 5.66–5.61 (m, 2H), 4.27, 4.07 (2d, J = 14.7 Hz, 2H), 4.97 (d, J = 8.1 Hz, 1H), 4.46 (dd, J = 6.5, 10.9 Hz, 1H), 4.24, 4.21 (2d, J = 8.7 Hz, 2H), 3.83 (d, J = 7.0 Hz, 1H), 3.39 (br s, 4H), 2.62–2.51 (m, 1H), 2.45 (s, 3H), 2.36–2.30 (m, 1H), 2.24 (s, 3H), 2.19–2.07 (m, 1H), 2.00 (s, 3H), 1.92–1.85 (m, 1H),

1.69 (s, 3H), 1.30 (s, 3H), 1.20 (br s, 6H), 1.15 (s, 3H). HRMS (FAB+): calcd for $C_{62}H_{66}N_2O_{14}$ [M^++Na]: 1149.4208, found: 1149.4202. Purity was higher than 95% (HPLC analysis at 230 nm).

21. Kazmierski, W. M.; Bevans, P.; Furfine, E.; Spaltenstein, A.; Yang, H. Bioorg. Med. Chem. Lett. 2003, 13, 2523.
22. Buck, K. B.; Zheng, J. Q. J. Neurosci. 2002, 22, 9358.
23. Bhat, N.; Perera, P.-Y.; Carboni, J. M.; Blanco, J.; Golenbock, D. T.; Mayadas, T. N.; Vogel, S. N. J. Immunol. 1999, 162, 7335.
24. Zhu, Q.; Guo, Z.; Huang, N.; Wang, M.; Chu, F. J. Med. Chem. 1997, 40, 4319.
25. Kingston, D. G. I. J. Nat. Prod. 2000, 63, 726.
26. Skwarczynski, M.; Sohma, Y.; Noguchi, M.; Kimura, T.; Hayashi, Y.; Kiso, Y. J. Org. Chem. 2006, 71, 2542.
27. Mizuta, H.; Watanabe, S.; Sakurai, Y.; Nishiyama, K.; Furuta, T.; Kobayashi, Y.; Iwamura, M. Bioorg. Med. Chem. 2002, 10, 675.
28. Zhu, Y.; Pavlos, C. M.; Toscano, J. P.; Dore, T. M. J. Am. Chem. Soc. 2006, 128, 4267.